A-Alkarim

Bin Raba

2010

Raindrop Size Distribution

MSc Wireless Systems Engineering

First Supervisor: Dr. Kevin S. Paulson

Second Supervisor: Mr. Nick G. Riley

ABSTRACT

One of the main impacts of climate change is leading to an increase in the incidence of heavy rain at outage level. In this thesis was to identify and study the impact of changes in raindrop size distributions (DSD) on the fixed terrestrial microwave links as a result of an increase in the incidence of heavy rain in the United Kingdom over this decade. Also to introduce an increasing trend in rain rates associated with outage. The daily DSD spanning was calculated from two different sites data (Chilbolton and Sparsholt), the data span up to 6 years at each site.

The attenuation that caused by heavy rain and rain drops is serious problem facing meteorologists and hydrologists. This thesis introduces to calculate the specific attenuation by using new method (power-low relationship). Also introduce the theory of scattering by such hydrometers as rain, snow, hail and fog. There are three techniques to determine the scattering parameters are Rayleigh Scattering, Mie Scattering and T-Matrix method.

ACKNOWLEDGMENTS

First of all, I would like to express my deepest gratitude to my first supervisor Dr. Kevin Paulson for his guidance throughout my graduate studies at Hull University.

I am also thankful to Mr. Nick Riley for his valuable and useful lectures that we have done throughout the academic year.

I am deeply grateful to my parents for their continuous support and encouragement

Finally, I would like to thank my friends for their great support.

TABLE OF CONTENTS

CHAPTER THREE: ATTENUATION AND RAINFALL

CHAPTER FOURE: SIMULATION RESULTS AND DISCUSSION

CHAPTER Five: CONCLUSION AND FURTHER STUDY

LIST OF FIGURES

LIST OF TABLES

CHAPTER 1

INTRODUCTION

1.1Introduction

Millimetre wave links offer large bandwidth and high speed communication for integrated multimedia services. Such links are also quick to deploy. This issue of greatest importance in the study of the performance of millimetre links is rainfall. In the design of such systems, the attenuation due to rain must be accurately accounted for in order to ensure system reliability and availability. Systems that are poorly designed lead to an increase in transmission errors, or worst, to an outage in the received signal.

1.1 Microwave Links

Microwave links or microwave transmission is an expression we use to refer to the technology of transmission information by using radio waves, when the wavelengths are small number of centimetres, by using versatile electronic technologies. The first hardware of microwave that used in the experiment was built by the Rutherford Appleton Laboratory to achieve the level of stability and reliability required for the experiment. The attenuation at each frequency was measured to about ± 0.5dB with a 40dB dynamic range. The probability of error is ± $1dB$ in the4 attenuation difference. In fact, the error in attenuation difference should be less than that at a single frequency, because the attenuation caused by rain is highly correlated (Rahimi et al., 2004). They carried out the test in urban link at the frequencies of 22.9 and 13.9GHz, and reached to the path does not pass close to the ground, buildings or other features. In contract, the microwave link does pass reasonably close to the ground and is therefore measuring the rain experienced at ground level.

1.2 The Effect of Climate Change on Rain in the UK

In the UK the effect of climate change can be seen as any other countries around the world. British coastal waters have warmed by about 0.7 degrees Celsius over the past three decades, this led to the rise in sea level around the UK is now about 10cm higher than it was in 1900. From began in 1766 when the rain amount recorded, the amount of winter rainfall in England and Wales has risen. Especially, in last 45 years it has become

heavier. The UK has the worst flood for 279 years in some areas was in 2000. Flood damage now costs Britain about £1 billion a year (Lawrimore et al., 2001).

Currently, the UK government spends in excess of £300 million annually on flood defences; this is likely to rise by another £200 million when also taking climate change impacts into account (Defra, 2001). Regarding UK trends in precipitation, UKCIP08 states that: "All regions of the UK have experienced an increase in the contribution to winter rainfall from heavy precipitation events. In summer all regions except NE England and N Scotland show decreases." Further states "A change of 5% in the contribution of heavy events (evident in most regions during winter) implies a change from a contribution of, say, 7.5% in the 1960s to a contribution of, say, 12.5% in the recent decade."

1.3 The Effect of Climate Change on Radio Communication in the UK

One of the main climate change impacts in the United Kingdom is an increase in rainfall, especially in the winter. According to Paulson (2010) the rain parameters are sensitive on the radio telecommunications networks at frequencies above 10 GHz is attenuation due to moderate and heavy rain, while other applications are not significant. The Office of Communications (Ofcom) which is spectrum regulation in the UK uses the map of 0.01% exceeded rain rate to calculate rain fade margins to set power levels for link licenses. Moreover, the rain rates (R) at the frequencies of interest is converted by raindrop size distributions into specific attenuation.

Also Paulson (2010) pointed out that the an increase interface in bands reliant upon Automatic Transmit Power Control (ATPC) as a result of increase in the incidence of heavy rain. Another effected of heavy rain that occurred on the satellite links. When the drops of water are high above the zero degree isotherms and so cause extreme attenuation on slant paths that pass within them.

1.4 Objectives

There are several objectives of this thesis:

- To understand hydrometeor attenuation on microwave links.
- To understand the effect of climate change on microwave telecommunications in the UK.
- Identify trends in Raindrop Size Distribution DSD associated with rain rates at outage levels.
- Finally, predict effects of DSD changes on microwave links.

1.5 Organization of Thesis

This thesis is organized as follows:

Chapter 1 begin with a study of the effect of climate change on microwave radio links, possibly this lead to changes in the number and duration of outage and availability on microwave greater than 10GHz links across the UK.

Chapter 2 introduce the background and literature review on raindrop size distribution (DSD), which is parameter that is of most interest.

Chapter 3 describes the attenuation and rainfall. The empirical specific attenuation provided by lTU-R838 will be used for the calculation of the attenuation and scattering theory. Also the attenuation that occurs as a result of absorption and scattering by such hydrometeors as rain,

Chapter 4 presents the results and discussion of the simulations and graphs to identify the trends of rain drops of the same rate. The data which were used in these programmes that read in Net CDF daily DSD files the variable of raindrop size from two sites.

Chapter 5 concludes the thesis with a summary of our work and suggestions for future investigation

CHAPTER 2

BACKGROUND AND LITERATURE REVIEW

RAINDROP SIZE DISTRIBUTION (DSD)

2.1 Introduction

The raindrop size distribution (DSD) describes the number and the size of the precipitation particles; also DSD reflects the distribution of the drop sizes as a function of the rain rate. These parameters are important in understanding the development and evolution of precipitation.

2.2 Rain

The main area that causes the formation cycle of clouds and causing rainfall is the lower troposphere, which extends at a height of 10 km from the earth's surface. The size of drop of rain in the beginning of the composition of $10\mu m$ and concentrations of $10^8 m^{-3}$, and condenses water vapour rising from the earth's surface. Melt ice crystals within the clouds in the form of drops of water, to become heavy enough to fall as rain. The process of rainfall occur by two mechanisms are the Bergeron process and collision/coalescence process (Lutgens and Tarbuck, 2001).

During their fall from clouds to earth's surface, small droplets may coalesce with each other forming bigger drops. Sometimes droplets are sounded by warm and dry air, and they may evaporate before reaching ground. In general, the rain consists of a distribution of drop sizes in the range of 0.5 mm to 10 mm. Fig 2.1 illustrates the cycle of rain beginning of the operation from the ground, and then precipitation in the lower troposphere to be drops of rain, and finally, the fall of rain to the earth again.

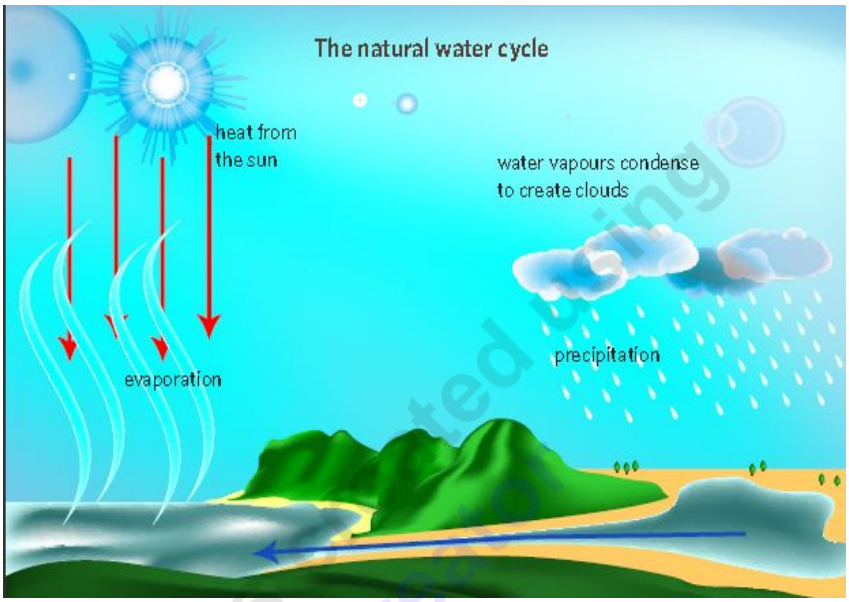

Figure 2.1: The cycle of rainfall formation.

(www.coralcoe.org.au/research/simonpng/EEPL)

2.3 Type of Rain

There are different types of rain with different spatial scales that range from a few kilometres in diameter to a few ten's of kilometres. Among these types, three major ones are convective, orographic and frontal (or stratiform) rainfall. The characteristics of these species in the first place, in the spatial extant, rain drop size and vertical movement of air, which plays a pivotal role in the formation of rain.

Convective rainfall is created when there is an abundance of moist air created by intense surface heating. The main area which the convective showers frequently occurred is tropical areas, where large clouds of warm moist air are carried inland from the sea. Also occur in summer months within temperate regions. In temperate climates, the upper limits in convective rain rates are between 100-150 mm/hr in Europe, whereas rain rates exceeding 200mm/hr in tropical climates.

Orographic rain occurs when air is forced to rise due to terrain features. When land areas such as mountain ranges lie in the path of extensive air masses.

As opposed to the vertical development of convective rain, frontal or stratiform rain is formed from stably stratified clouds. Stratiform clouds are horizontally widespread (can extend more than 100-1000 km) and protracted. In stratiform clouds, precipitation grows in a widespread forced updraft of low magnitude. Stratiform rain typically varies between 0.2-10 mm/hr, with the upper limit being exceeded only very rarely. Raindrops form in stratiform clouds primarily by condensation. Because of a lake of a strong updraft to keep droplets aloft, stratiform rain falls out of the cloud with lower rain rate. Stratiform rain is more uniform in intensity and consists of relatively small raindrops.

2.4 Raindrop Size Distribution (DSD)

The research since the 1940s has focused on the analysis description of the drop water. According to Laws and Parsons (1943) the drop size was obtained by using the technique of counting the drops failing in un-compacted flour, and the tables of DSD measurements was produced. The first analytical description of DSDs was presented by Marshall and Palmer (1948).

Rain comprises drops of many different diameters, which are characterized by a particular raindrop size distribution (DSD) that provides information on the number and size of raindrops in a simple. Because the DSD is a unity area distribution, calculated at different resolutions gives different curves, which can be seen in figure 2.2. If all the drops fall at their terminal velocity in still air, the rainfall rate (mm/h) is related to the DSD the following equation,

$$R = C \int_{D_{min}}^{D_{max}} D^3 v(D) N(D) dD, \qquad (2.1)$$

Where N(D) is the drop size distribution, D is the drop size, $v(D)$ is the terminal velocity of drops falling in air and C is a constant whose value depends on the units of measurement of the parameters.

Choosing the same rain rate, different scale of drop size interval defines a different probability density function (pdf) of DSD within a unit volume. Thus DSD, usually denoted by $N(D)$ with units of m^{-4} is a fundamental quantity used to describe the characteristic of rain.

Only the M-P and Weibull DSD's will be considered in the derivation of specific attenuation. The M-P DSD is chosen because it is widely accepted, although is found to

overestimate the number of small drops (Olsen, 1978). The Weibull DSD is chosen because it was found to yield the least rms error with experimental data as opposed to the other mentioned distributions (Jiang, 1997).

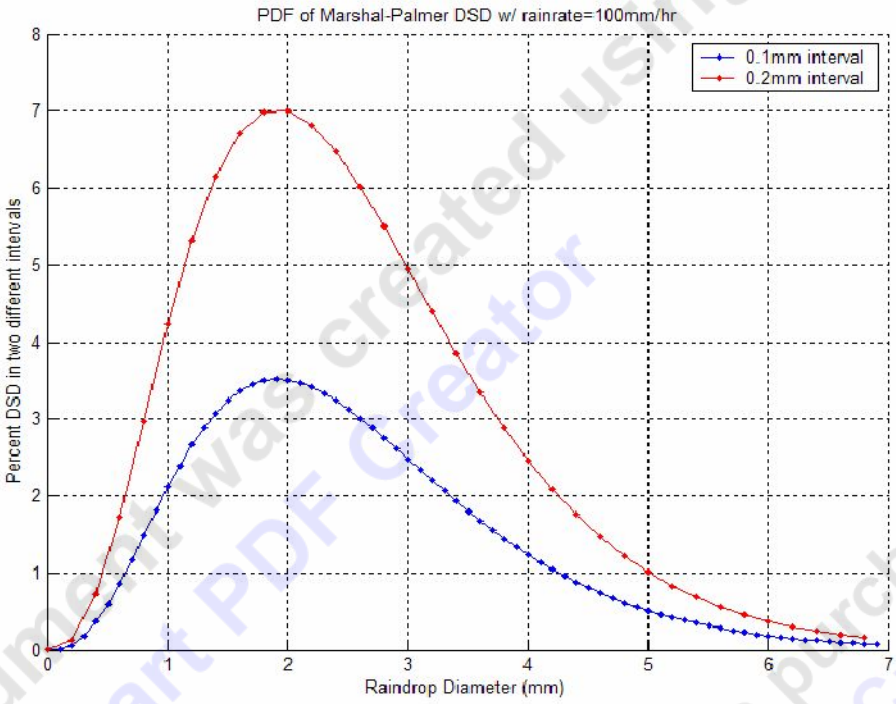

Figure 2.2 PDF of Marshal-Palmer DSDs with diameter interval 0.1 mm and 0.2mm

(FANG FANG, 2003)

2.4.1 Marshall–Palmer DSD

The raindrop size distribution has been studies by many investigators and generally modelled as an exponential distribution. The most widely used DSD in scientific literature is Marshall and Palmer, which is a special case of the exponential distribution with two fitting parameters N_0 and Λ. Marshall- Palmer DSD is defending as:

$$N(D) = N_0 e^{-\Lambda D}, m^{-4} \qquad (2.2)$$

Where $N_0 = 8 \times 10^6 \, m^{-4}$, Λ is the slope parameter. It is related to rain rate R (mm/hr) as:

$$\Lambda = 41R^{0.21}, m^{-1} \qquad (2.3)$$

The M-P radar reflectivity Z-R relation is given by:

$$z = 200R^{1.6} \qquad (2.4)$$

2.4.2 Weibull DSD

The Weibull drop size distribution (Sekine, 82) is expressed as:

$$N(a_0) = N_0 \frac{\eta}{\sigma} \left(\frac{2a_0}{\sigma}\right)^{\eta-1} e^{\left\{-\left(\frac{2a_0}{\sigma}\right)^{\eta}\right\}} \quad m^{-3}mm^{-1} \qquad (2.5)$$

Where the precipitation rate R is in mm/hr and

$$N_0 = 1000 \quad m^{-3}$$

$$\eta = 0.95R^{0.14}$$

$$\sigma = 0.26R^{0.42} \quad mm$$

The Weibull reflectivity Z-R relation is given by (Jiang96):

$$Z = 285R^{1.48}$$

2.5 Rain Rate (R)

Rain rate R is a measure of the intensity of rain by calculating the volume of rain that falls to ground in a given interval of time. The rain rate is expressed in units of length (depth) per unit time (mm/hr), which is the depth of rain captured in a collection vessel per unit time. Figure 2.3 illustrates a graphical representation of pdf of Marshall-Plamer DSD with three different rain rates. The drop size increases, As a result of a rain intensity increase. Under stratiform rainfall conditions, the vertical air motion is weak and is usually neglected because its value is generally not known. The error introduced is believed to be small compared to terminal velocity of most rain drops. Rainfall rate R is related to $N(D)$ (Williams, 2002).

$$R = \frac{6\pi}{10^4} \int_0^{\infty} v(D) D^3 N(D) dD, \qquad \text{mm/hr} \qquad (2.6)$$

An exponential of fall speed to diameter relationship is derived as:

$$v(D) = [\alpha_1 - \alpha_2 \exp(-\alpha_3 D)] \left(\frac{\rho_0}{\rho}\right)^{0.4}, m/s \qquad (2.7)$$

Where α_1= 9.65 m/s, α_2=10.3 m/s, and α_3=0.6m/s. $\left(\frac{\rho_0}{\rho}\right)^{0.4}$ is a density ratio factor adjusting terminal fall speed due to air density change with altitude.

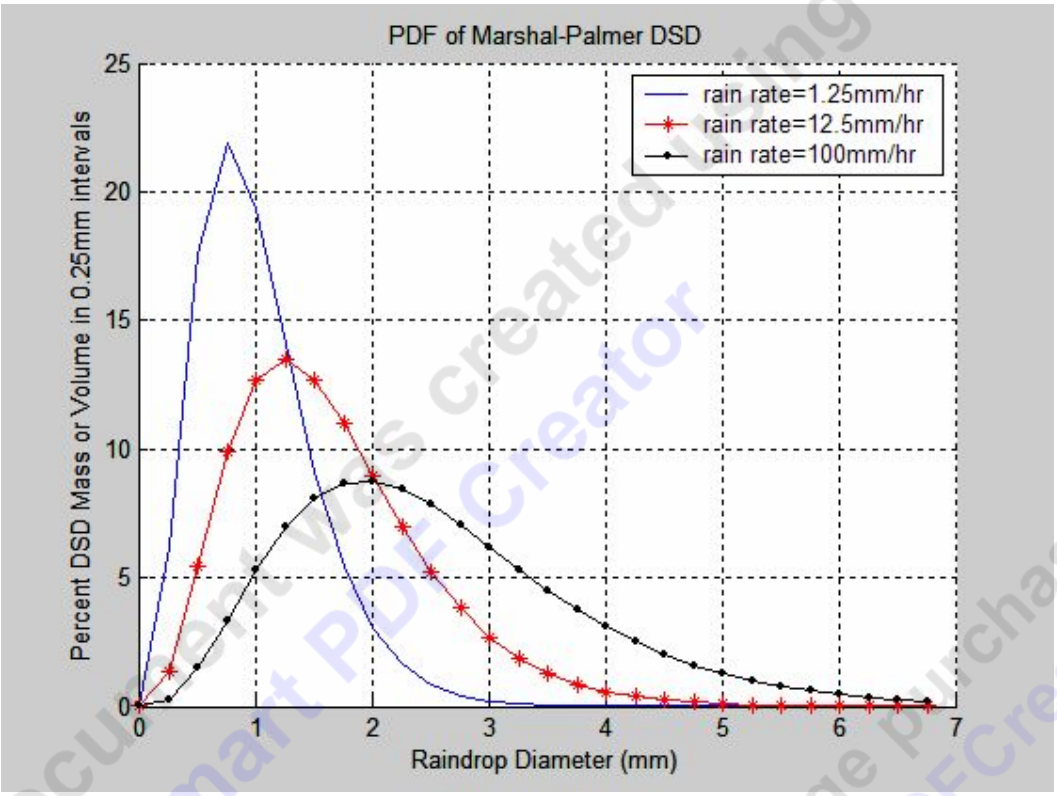

Figure 2.3 PDF of Marshall-Palmer DSDs with Three Different Rain Rates

(FANG FANG, 2003)

2.6 Gamma Distribution

There is a three parameter distribution yields a better approximation to empirical distributions than the two parameter M-P DSD (Atlas & Ulbrich, 1984). Ulbrich (1983) has remarked that from measurements of drop size spectra, that Gamma distribution of the form ,

$$N(D)dD = N_0 D^{\mu} \exp(\Lambda D)\, dD \qquad (0 \le D \le D_{max}), \qquad (2.8)$$

Where μ describes the breath of the distribution and mostly varies in the range -1 to 10 from physical observations [Tokay & Short 1996].

2.7 Raindrop Shape

Raindrops range in size from the very small to the fairly large in the range 0.5-10mm in diameter, with drops greater than 8mm being hydro-dynamically unstable and breakupas they fall. There are three different raindrop shapes that will be considered. The spherical and spheroidal shapes are axisymmetrical about the horizontal axis (Oguchi,1977). While the Pruppacher and Pitter shape is distorted. The Pruppacher and Pitter model is more realistic than first two mentioned. The raindrop starts almost spherical, then becomes spheroidal and axisymmetricfor midsize raindrops, and finally becomes distorted and nonaxisymmertric. This leads to the use of the model in heavy rain climates due to the increased presence of larger raindrops. The drop size which is produced from convective rain is wider range than stratiform rain but there is no relationship between the rainfall types produced and size distribution of drops.

The drops fall faster as a result of increasing in drop size, and the surface drag due to air resistance has an increasing effect on the drop shape. For the drops large than 1mm diameter are oblate with much larger drops having a concavity on the base. The shape of drops with varying size is given in Figure 2.4.

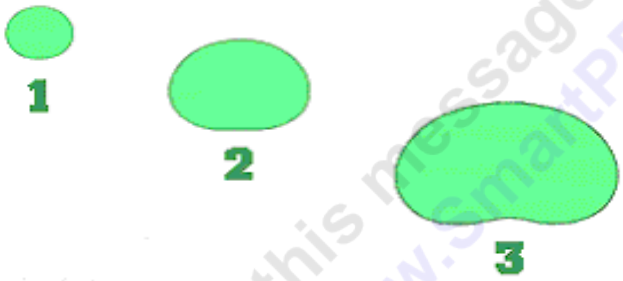

Figure 2.4 Rain drop shapes with the numbers below indicating their equi-volumetric radiiin millimetres. (Isa. Usman, 2005)

Two studies have carried out the measurements of drop shape by using photographs of water drops suspended in a wind tunnel (Pruppacher & Beard 1970). They illustrated that water drops falling at terminal velocity were deformed into oblate spheroids. Also they found a linear relationship between the axial ratios and drop size at the range of 1-4mm. The empirical expression is given by,

$$\frac{b}{a} = 1.03 - 0.62D, \qquad (2.9)$$

Where a and b are the minor and major axes of the drop respectively. This relationship is only valid when the drop sizes are greater than 1mm. Another linear relationship was carried out later by Morrison & Cross (1971), depend upon the analysis of electromagnetic wave scattering by raindrops. This is given by:

$$\frac{b}{a} = 1.0 - 0.5D. \qquad (2.10)$$

Two researcher Beard & Chuang (1987) have shown that the linear model of equation 2.9 overestimates the axis ratio for large drops (> 4mm). This was motivated by increased interest to evaluate the effect of depolarisation, which causes cross-polar interference.

$$\frac{b}{a} = 1.005 + 0.0057D - 2.268D^2 + 3.682D^3 - 1.677D^4 \qquad (2.11)$$

The correction to the axis ratios of Beard & Chuang for small drops has been made. This was based on the discrepancy between disdrometer measurements compared with observations of integrated rainfall measurements using polarisation radar (Goddard & Cherry, 1984). They provide a polynomial expression given by,

$$\frac{b}{a} = \{1.075 - 0.065D - 0.036D^2 + 0.04D^3 \quad D \geq 0.11\ cm \qquad (2.12)$$

$$\frac{b}{a} = \{1.0 \qquad D < 0.11\ cm \qquad (2.13)$$

In further, wind tunnel experiments by Andasager et al. (1999) produced a polynomial model that agreed well with equation (2.15) and given by,

$$\frac{b}{a} = 1.012 - 0.144 - 1.028D^2 \qquad (2.14)$$

CHAPTER 3

ATTENUATION AND RAINFALL

3.1 OVERVIEW OF ATTENUATION PREDICTION

The primary goal of a rain attenuation prediction method is to achieve acceptable estimates of the attenuation incurred on the signal due to rain, given the system requirements such as frequency, path length, polarization, path geometry, rain rate distributions, and availability. The International Telecommunication Union (ITU) prediction model (ITU530) is a first point of reference for engineer. Improvements to the models come from measurement programs which provide further insight into the physics of precipitation systems and also data against which their accuracy can be evaluated.

A power law empirical relation between the specific attenuation and the rain rate has been found to be a good approximation (Olsen, 1978). The derivation of the specific attenuation is a known result from scattering theory, but the computation is complicated using the perturbation method (Oguchi, 1960), because it involves the summation of spherical Bessel functions and associated Legendre functions. Therefore, the empirical relation for evaluating the specific attenuation is extremely practical, since the parameters are given in a tabulated form and calculations can be carried out in seconds.

The path attenuation was first calculated (Lin, 1975) by directly applying the line rain rate in the empirical relation previously discussed. Later Crane (Crane, 1980) found a power low relation between the line rain rate and point rain rate from which he evaluated the instantaneous rain profile. He then utilized the empirical relation between the attenuation and rain rate to compute an exponentially fitted effective path length. The attenuation along the path is then obtained by multiplying the specific attenuation by the computed effective path length.

The purpose of this chapter is to analyse the electromagnetic scattering by rain drops because rain is the most important precipitation in our climatic conditions Rain consists of rain drops of various diameters from 0.01 to 0.7 cm and various frequency (DSD).

The proposed model is based on existing International Telecommunication Union Radiocommunication Sector (ITU-R) recommendations methods where appropriate; this will help to gain acceptance within the ITU-R community. The current methods for terrestrial and earth space have been extracted from their associated recommendations.

The model is smooth and applicable to all time percentages 0-100%. When there is no rain there is no rain attenuation. When rain does occur the rain rate will not be uniform along the entire path. In order to obtain the parameters for the formula, specific attenuation at different rain rates, calculated from theoretical models. The ITU-Recommendation 838 [ITU838] has become the standard for this specific attenuation estimation.

3.1.1 ITU-R838 Specific Attenuation Model for Rain

The specific attenuation is computed by using the following power-low relationship:

$$\gamma_R = kR^{\alpha} \qquad (3.1)$$

Where γ_R is the specific attenuation in dB/km and R the rain rate in mm/h.

The frequency dependent coefficients k and α are given in the table 3.1 for vertical and horizontal linear polarizations, and terrestrial paths.

The values of k and α given in ITU-R P.838-3 are considered to be universally applicable. It is important to note that this is a gross approximation, one that has been tested to give good results in the UK at the 99.99% availability level, which corresponds to rain rates of around 20-30mm/hr. In practice both k and α vary considerably with type of rain, specifically the drop sizes, the drop shapes and orientation relative to the plane of polarisation and with the temperature of the rain.

Then, the log specific attenuation may be written as:

$$\Gamma = \ln(k) + \alpha X(t) \qquad \ln(\text{dB/km}) \qquad (3.2)$$

For all other path geometries and polarization, the coefficients in above equation can be calculated from the values in Table 3.1 by using the following equations:

$$k = \frac{[k_H + k_V + (k_H - k_V)\cos^2\theta\cos 2\tau]}{2} \qquad (3.3)$$

$$\alpha = \frac{[k_H\alpha_H + k_V\alpha_V + cos^2\theta cos2\tau]}{2k} \qquad (3.4)$$

Where θ is the path elevation angle and τ is the polarization tilt angle relative to the horizontal, e.g., circular polarization $\tau = 45^o$.

Table 3.1 - Selected k and α from P838-3

Frequency (GHz)	k_H	α_H	k_V	α_V
1	0.0000259	0.9691	0.0000308	0.8592
3	0.0001390	1.2322	0.0001942	1.0688
5	0.0002162	1.6969	0.0002428	1.5317
7	0.001915	1.4810	0.001425	1.4745
10	0.01217	1.2571	0.01129	1.2156
12	0.02386	1.1825	0.02455	1.1216
15	0.04481	1.1233	0.05008	1.0440
20	0.09164	1.0568	0.09611	0.9847
22	0.1155	1.0329	0.1170	0.9700
23	0.1286	1.0214	0.1284	0.9630
24	0.1425	1.0101	0.1404	0.9561
25	0.1571	0.9991	0.1533	0.9491
30	0.2403	0.9485	0.2291	0.9129
35	0.3374	0.9047	0.3224	0.8761
40	0.4431	0.8673	0.4274	0.8421
45	0.5521	0.8355	0.5375	0.8123
50	0.6600	0.8084	0.6472	0.7871

(Report on Modelling of Rain Attenuation, 2008)

According to the Report on Modelling of Rain Attenuation (2008), the difference in specific attenuation that results from using the rain rate distribution, as modelled for the UK and method in P.530-12. In two graphs below were based on a 0.01% rain rate of 20mm/hr which is reasonable for the UK.

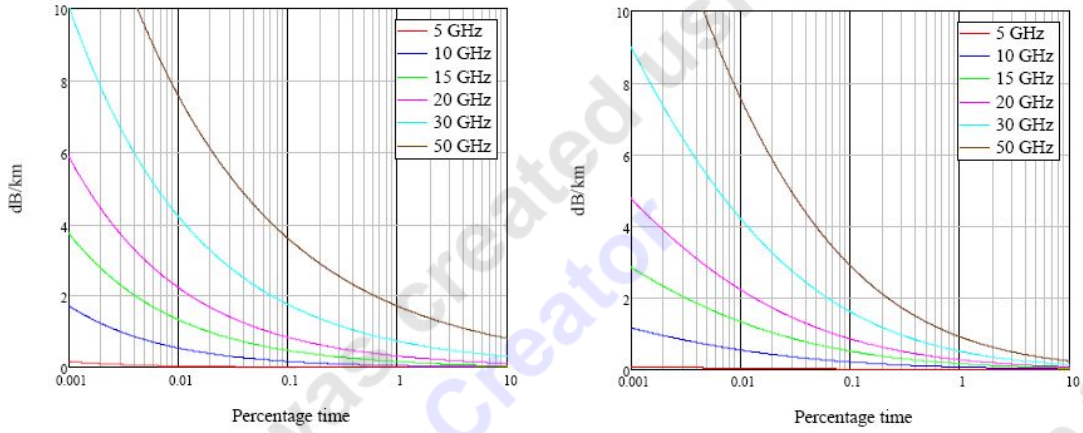

Based on Rain Rate Based on 0.01%

Figure 3.1 – Specific attenuations based on rain rate distribution and P530-12

(Report on Modelling of Rain Attenuation, 2008)

3.1.2 Attenuation and Rainfall

The transmitted wave will be attenuated, as a result of impinges on region of hydrometeors when an electromagnetic wave of wavelength λ and wavenumber $k_0 = \frac{2\pi}{\lambda}$, while energy will be scattered and absorbed by the hydrometeors (Hulst, 1981). Let the number of drops with equivolume diameter in the range $(D, D + dD)$ is $N(D)dD$, and that the (complex) forward scattering amplitude for scattering by a drop of diameter D is $f(D)$. Then with

$$A = 8.686 \times 10^5 Im^{-1}(k) \qquad (3.5)$$

Where D and f are in cm, k and k_0 are in cm^{-1} and $N(D)$ is in cm^{-4}.

Altas and Ulbrich (1977) show that the relationship between rainfall and attenuation a near linear at 35 GHz, while other author Jameson (1991) illustrates that the relation at 25

GHz is even closer (with rain rate proportional to attenuation raised to the power 0.99) and is unaffected by variations in the raindrop size distribution. Jameson considered the measurement errors to be expected on a 1km link and concluded that the attenuation at theses frequencies would be a useful for path averaged rain rate in excess of 1mm/hr, also he has noted that at three different frequencies 9 GHz, 25GHz and 38GHz the attenuation difference were capable of providing useful estimates. Later Rincon and Lang (2002) have been confirmed that a dual frequency microwave link experiment using 25 GHz and 38GHz with a 2.3 km link. The attenuation difference could be useful for measuring rainfall as many of authors have been noted within an experiment monitoring the 12.5 GHz and 19.8 GHz data from the Olympus Satellite (Hardaker et al., 1997).

It should be noted that precipitation along a path may not be rain alone, but could be hail, or, when the temperature is low enough, sleet or snow. Attenuation in snow is negligible. Attenuation in sleet can be substantially greater than in rain and the method then over estimates the amount of precipitation (though our recent research suggests that we can detect this occurs in the link data)

3.2 Attenuation due to hydrometeors

Attenuation can also occur as a result of absorption and scattering by such hydrometeors as rain, snow, hail and fog**.** Even though the rain attenuation can be ignored at frequencies below about 5 GHz, it must be included in design calculations at higher frequencies, where its importance increases rapidly.

3.2.1 Scattering Parameters

Any type of electromagnetic wave propagating through the atmosphere is affected by the aerosols because of their interaction with radiation. The interaction fall into three categories:

(i) Scattering

(ii) Absorption

(iii) Emission.

Scattering is the result of interaction between light and particulate matter and occurs at all wavelengths in the electromagnetic spectrum. The re-distribution of incident energy

during scattering depends strongly on the ratio of particle size to wavelength of the incident wave. If the particle is isotropic, the scattering pattern is symmetric about the direction of incident wave.

Small particles with sizes very small compared to the wavelength of incident radiation, scatter almost equally into both the forward and backward direction. As the particle size becomes comparable with the wavelength of incident radiation more energy is scattered in the forward direction and secondary maxima and minima appear at various angles. However the overall scattering increases with the increase in size of the particle and ultimately depends upon the ratio of refractive index of the particle relative to that of the surrounding medium.

When scatterers are very small compared to the wavelength of incident radiation ($r < \lambda/10$), the scattered intensity on both forward and backward directions are equal. This type of scattering is called Rayleigh scattering. In this type of scattering, the scattered intensity varies inversely as the fourth power of wavelength.

When scatterers are larger particles ($r > \boldsymbol{\lambda}$), the angular distribution of scattered intensity becomes more complex with more energy scattered in the forward direction. This type of scattering is called Mie scattering.

In Rayleigh and Mie scattering, both the scattered and incident radiation have the same wavelength and hence this two scattering process are called Elastic scattering.

Another type of scattering in the scattering problem of elastic waves, the wave function extension method plays a basic and important role. When the scatterer is a circle cylinder, an elliptical cylinder, a sphere and a spheroid the scattering problem of elastic waves can be solved by the wave function extension method meets a difficulty. Then the T-matrix method of elastic wave scattering was proposed. The advantage of T-matrix method is that it can be used to deal with arbitrary shape. However, the traditional T-matrix method is applied to perfect interface; namely.

There is no different mechanisms between Rayleigh and Mie scattering, they have a simply models approximating and the scattering mechanism applicable at different wavelength. It can see that from the following diagram, scattering does not just affected radiowaves, scattering of light in the air is why the sky is not black.

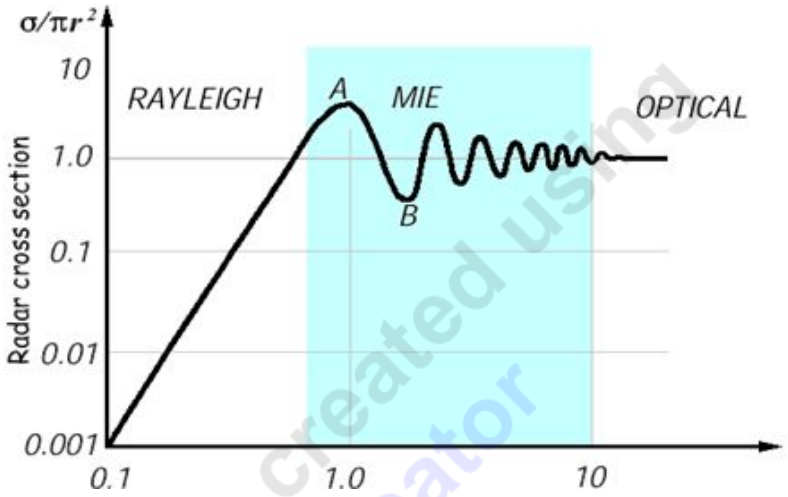

Figure 3.2 Particle diameters in wavelengths

(David W. Hahn, 2009)

In order to predict the effects of rain scatter on a propagating electromagnetic wave, the scattering parameters of individual raindrops must be determined. There are three techniques for doing this are Rayleigh Scattering, Mie Scattering and T-Matrix method.

3.2.1.1 Rayleigh Scattering

The scattering of light by gases was first treated quantitatively by Lord Rayleigh in 1871 in an effort to explain the blue colour of the sky and the red colour of the sunset. Rayleigh scattering theory could explain the blue colour of the sky.

A small homogeneous was considered, isotropic particle whose radius is much smaller than wavelength of the incident radiation. The incident radiation produces an electric field E_0, called applied field. Since the scatterers are very small compared to the wavelength, the applied field generates a dipole configuration on it. Now let E be the combined field, the applied field plus the particles own field.

If P_0 is the induced dipole moment, then

$$P_0 = \alpha E_0 \qquad (3.6)$$

Where α is the polarisability of the small particle. The dimension of E_0 is charge per area and P_0 is charge times length and hence α has dimension of volume.

The applied field E_0 generates oscillation of an electric dipole in fixed direction. The oscillating dipole, in turn, produces a plane polarised electromagnetic wave, the scattered wave.

If we consider the distance between the dipole and observation point is r, the angle between the scattered dipole moment P and the direction of observation is γ, and the velocity of light is c.

According to Hertz low, the scattered electric field is proportional to the acceleration of the scattered dipole moment and sin γ and inversely proportional to the distance r.

$$E = \frac{1}{C^2}\frac{1}{r}\frac{\partial^2 P}{\partial t^2} sin\gamma \qquad (3.7)$$

In an oscillating periodic field, the scattered dipole moment can be written in terms of induced dipole moments as:

$$P = P_0 e^{-ikr(r-ct)} \qquad (3.8)$$

Where k is the wave number, and $kc = \omega$ is the circular frequency.

By combining the two equations,

$$E = -E_0 \frac{e^{-ik(r-ct)}}{r} k^2 \alpha \sin\gamma \qquad (3.9)$$

Consider the scattering by air molecules in the atmosphere.

Let the plan defined by the direction of incident and scattered waves are the reference plane (plane of scattering).

Since any electric vector may be arbitrarily decomposed into orthogonal components, two components, perpendicular (Er) and parallel (El) to the scattering plane are considered here

Assuming air molecules to homogeneous, isotropic spherical particles,

$$E_r = -E_{0r} \frac{e^{-ik(r-ct)}}{r} k^2 \alpha \sin\gamma_1 \qquad (3.10)$$

$$E_l = -E_{0l} \frac{e^{-ik(r-ct)}}{r} k^2 \alpha \sin\gamma_2 \qquad (3.11)$$

From the scattering geometry, it can be seen that

$$\gamma_1 = {}^{\pi}/_{2} \qquad (3.12)$$

And

$$\gamma_2 = \pi/2 - \theta \qquad (3.13)$$

Where θ is defined as the scattering angle, which is the angle between the incident and scattered waves.

Here γ_1 is always 90^o because the scattered dipole moment in the r direction is normal to the scattering plane.

The corresponding intensities (per unit solid angle $\Delta\Omega$) is given by:

$$I_0 = \frac{1}{\Delta\Omega}\frac{C}{4\pi}|E_0|^2 \qquad (3.14)$$

and

$$I = \frac{1}{\Delta\Omega}\frac{C}{4\pi}|E|^2 \qquad (3.15)$$

Combining the two equations,

$$I_r = I_{or}K^4\alpha^2/r^2 \qquad (3.16)$$

$$I_l = \frac{I_{ol}K^4\alpha^2}{r^2 cos^2\theta}/r^2 \qquad (3.17)$$

Where I_r and I_l are the polarised intensity components perpendicular and parallel to the plane containing incident and scattered waves, for example, plane of scattering.

The total scattered intensity of unpolarised sun light incident on molecules in the direction θ is then:

$$I = I_r + I_l = (I_{or} + I_{ol}cos^2\theta)K^4\alpha^2/r^2 \qquad (3.18)$$

For unpolarised sunlight:

$$I_{or} = I_{ol} = I_0/2 \qquad (3.19)$$

and

$$k = 2\pi/\lambda \quad (3.20)$$

$$I = \frac{I_0}{r^2}\alpha^2 \left(\frac{2\pi}{\lambda}\right)^4 \frac{1+cos^2\theta}{2} \quad (3.21)$$

This is the formula derived by Rayleigh.

The scattered intensity depended on the wavelength of incident and the index of refraction of air molecules contained in the polarisabiltiy term.

$$I_\lambda \sim \frac{1}{\lambda^4} \quad (3.22)$$

A large portion of the solar energy is contained in the visible spectrum from blue ($\sim 0.425\ \mu m$) to red ($\sim 0.65 \mu m$).

According the equation for intensity, the blue light scatters are about 5.5 times more than red light. Also apparent that the ($1/\lambda^4$) dependence causes more blue light to be scattered than the red, green, yellow etc. therefore, we see the sky from a distance appears blue.

3.2.1.2 Mie Scattering

Mie scattering is caused by many different ways such as: pollen, dust, smoke, water droplets, and other particles in the lower portion of the atmosphere. Also called Lorenz-Mie-Debye theory or Lorenz- Mie theory. In 1908, the German physicist Gustav Mie formulated a complete scattering /abortion theory, which describe the interaction of electromagnetic waves with spherical dielectric particles. He illustrated a solution could be found given in terms of an infinite series of electric and magnetic multipoles.

The Mie approximation will enable to simplify various considerations and calculations. The Mie scattering approximation by depending of rain attenuation is enables to study the frequency and temperature, but unfortunately that approximation excludes the analyses of depolarisation phenomena. It is usually published in the next form of infinite series

$$f = \frac{j\lambda^3}{\pi^3 D^2}\left[\sum_{n=1}^{\infty}(2n+1)(a_n + b_n)\right] \quad (3.23)$$

Where a_n *and* b_n are the Mie's coefficient, and D is equivolumetric rain drop radius.

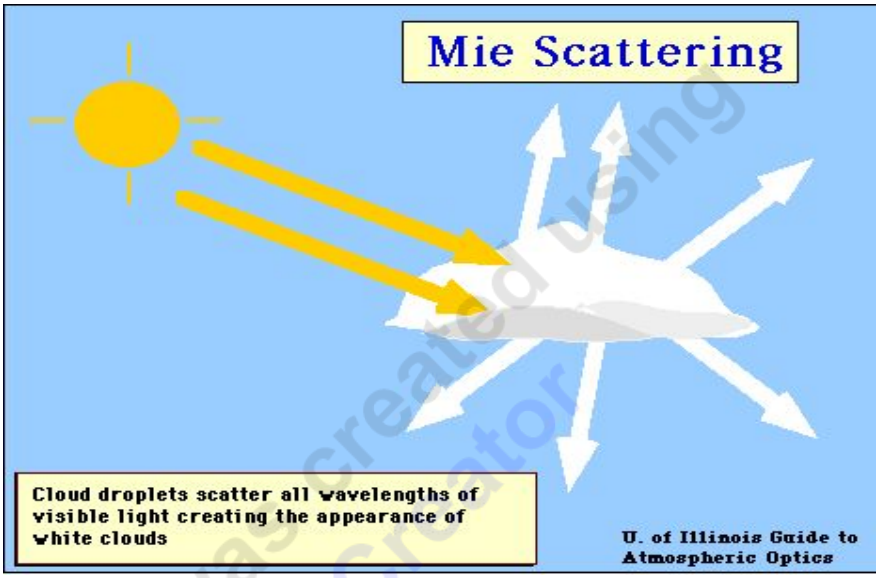

Figure 3.3 Mie scattering graphic (www.everythingweather.com)

3.2.1.3 T-matrix method

T-matrix method or as also called the Entended Boundary Condition Method (EBCM) is one of the most powerful and wildly techniques based on the linearity of Maxwell's equations that used for the calculation and to determine the effect of rain scatter on propagation electromagnetic wave. Since 1965, the T-matrix method has become one of the most of the powerful and popular theoretical for treating electromagnetic.

The main advantage of T-matrix method is that calculation can be made with very high efficiency. Another important feature of the T-matrix theory is that the symmetries of scattering particles may be taken into account. This results in substantial simplifications in making computations.

The major consideration in the design of microwave radio systems are rain induced attenuation and depolarization. However, to predict the signal degradation that will result from a rain event, determining the scattering properties of individual raindrops.

The purpose of this part is to present the how individual raindrop scattering parameters can be used to predict the attenuation and depolarization caused by a distribution of raindrops.

We consider scattering of a plane electromagnetic wave having wavenumber k by a single homogeneous particle of irregular shape, and plane parallel slab of raindrops which is illuminated by plane wave propagating in the z direction. The raincell is of indefinite extent and length d and the incident wave has as its electric field vector.

$$\overrightarrow{\bar{E}_i}(z) = \overrightarrow{\bar{E}_0} e^{-jkz} \qquad (3.24)$$

$$\overrightarrow{\bar{E}_0} = xE_{0x} + y\bar{E}_{0y} \qquad (3.25)$$

It can be shown that the coherent (average) field at a point z within tah rain cell is given in matrix form by

$$< E(z) > = e^{-jk(z)} E_i(z) \qquad (3.26)$$

Where

$$< E(z) > = [< E_x(z) > < E_y(z) >]^T \qquad (3.27)$$

$$\bar{E}_0 = [E_{0x} E_{0y}]^T$$

$$k(z) = 2\pi k^{-1} \int_0^z \int_\omega f(\check{z}, \check{z}, \vec{\omega}) \rho(z, \vec{\omega}) d\vec{\omega} dz \qquad (3.28)$$

$where$, ω is a vector of the random properties of individual raindrop (e.g. size, shape and canting angle), $f(\check{z}, \check{z}, \omega)$ the tensor forward scattering amplitude of raindrop having properties ω and $\rho(z, \omega)$ is the number of drops per unit volume in class ω. The matrix exponential $e^{-jk(z)}$ can be evaluated using the Cayley Hamilton theorem after the matrix $k(z)$ is determined through numerical quadrature. The attenuation and depolarization caused by the slab of raindrops can be estimated.

To determine the scattering properties of an individual raindrop, we consider a unit plane wave illuminates an oblate spheroidal raindrop and the incident field, $E_i(r)$, is given by

$$\overrightarrow{E_i}(r) = \overrightarrow{E_1}(r) \; or \; \overrightarrow{E_2}(r) \qquad (3.29)$$

$where$

$$\overrightarrow{E_1}(r) = (x\cos\ \square - \check{z}\sin\ \square)$$

$$= \exp[-jk(x\sin\ \square + z\cos\ \square)]$$

$$\overrightarrow{E_2}(r) = \hat{y}\exp\ [-jk(x\sin\ \square + z\cos\ \square)]$$

The objective of the T-matrix method is to express this scattered field in terms of the incident field and the size and dielectric properties of the raindrop. This goal is accomplished in the several steps:

First, the original scatterer is replased by surface current densities $J\ \square_+$ (electric) and $\vec{M}_+$ (magnetic) where

$$J\ \square_+ = \check{n}x\ (\overrightarrow{H_i}+\overrightarrow{H_s}) = \check{n}x\overrightarrow{H_+} \qquad (3.30)$$

$$\vec{M}_+ = \left(\overrightarrow{E_i} + \overrightarrow{E_s}\right)x\check{n} = \overrightarrow{E_+}x\check{n} \qquad (3.31)$$

and $\check{n}$ is the normal unit vector on σ, the surface enclosing the original scattering volume. $\overrightarrow{E_i}(\overrightarrow{E_s})$ and $\overrightarrow{H_i}+(\overrightarrow{H_s})$are respectively, the incident (scattered) electric and magnetic fields outside of σ.

The total field anywhere is the sum of the incident field and the scattered field, $E(r)$ must be equal and opposite the incident field inside of σ,

$$\overrightarrow{E_s}\ (\overrightarrow{r}) + \vec{E}_i(\overrightarrow{r}) = 0, \vec{r}\ wit\square in\ \sigma \qquad (3.32)$$

In addition to this, the tangential fields must remain continues across the surface of the scatterer, which was denoted as S:

$$\check{n}x\overrightarrow{E_t} = \check{n}x\overrightarrow{E_+} \quad \text{on S} \qquad (3.33)$$

$$\check{n}x\overrightarrow{H_t} = \check{n}x\overrightarrow{H_+} \quad \text{on S} \qquad (3.34)$$

Where $\overrightarrow{E_t}$ and $\overrightarrow{H_t}$ are the fields internal to the scatterer.

CHAPTER 4

SIMULATION RESULTS AND DISCUSSION

4.1 Introduction

This chapter presents the results and discussion of the simulations and graphs. The data which was used in these programmes that read in Net CDF daily DSD files the variable of raindrop size from two sites. The data that provided from the first site Chilbolton are from 2003 until the first three months of this year 2010. The data from the other site Sparsholt are from 2004 also until the first three months from this year 2010.

Firstly, a drop size distribution for each year was simulated to illustrate the histogram of DSD for daily and annual. Secondly, all these years were combined and simulated to illustrate the time series of the annual number of large raindrops and time series of the proportion of year spanned by the data. Thirdly, two tests Mann-Kendall and Pearson Correlation Coefficient were used to identify the trends of rain drops for the same rate. Finally, the average of DSD for each rain rate was given trends and probability for Mann-Kendall and Pearson Correlation Coefficient tests.

4.2 Annual and Daily Drop Size Distribution

The data from each site are used in first program separately to calculate daily and annual DSD, by using Chilbolton site data which was started from 2003 until March 2010. The daily and annual drop size distribution was different from day and year to others. It can be seen that some of days did not have any result for simulated of drop size distribution, as shows in Figure 4.1 below that means there is no rainfall in that day. Three random years were selected as an example to illustrate daily and annual DSD. The data which was simulated from the one day of year for 2003, the data are from 0 mm to 5 mm in raindrop diameter and from − 1 to + 1 in daily drop count.

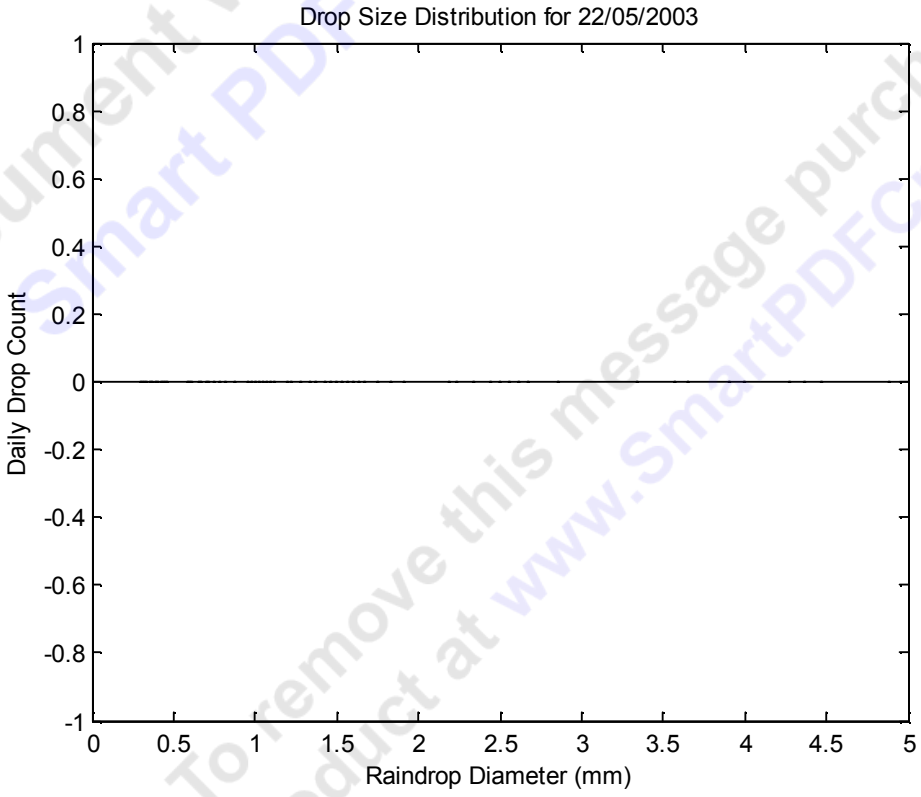

Figure 4.1 Drop Size Distribution for (22/05/2003)

Also rain diameter is depended upon if the rain is light rain or heavy rain, light or drizzle rain means that the size of drops did not exceed more than 1mm, while the size of drops resulting from heavy rain exceed 5 mm.

In the Figure 4.2 is for the year of 2003 which has data missing for first three month of that year, the data are from 0mm to 5mm in raindrop diameter and from 0×10^5 to 3.5×10^5 in Annual drop count. It is clear to see that the large amount of rain that fell as the light shower when the raindrop diameter was smaller than 1mm.

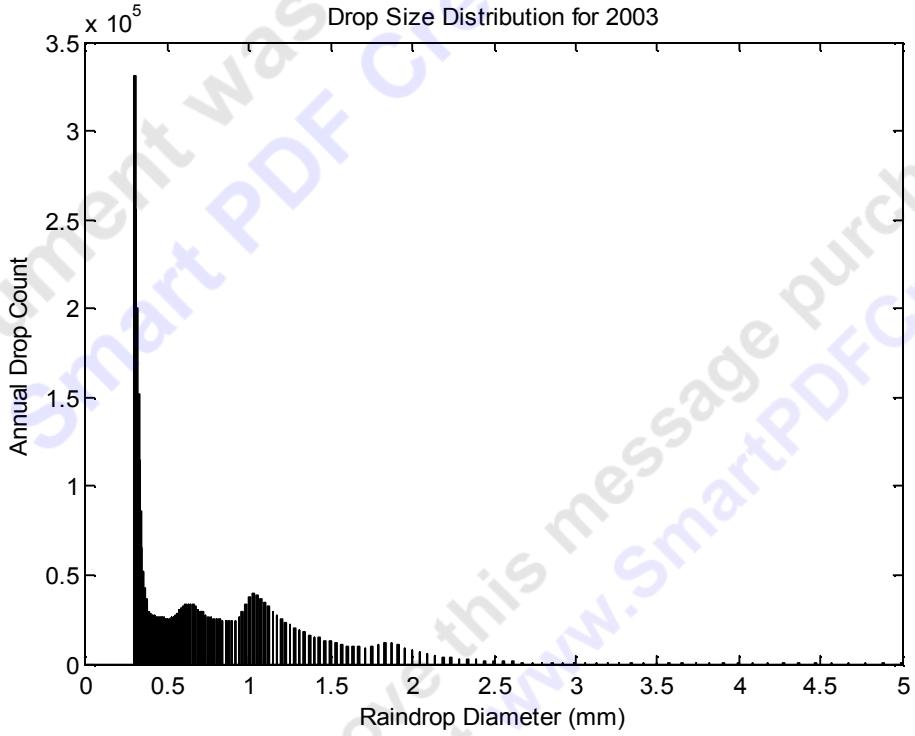

Figure 4.2 Drop Size Distribution for the year of 2003

Figure 4.3 illustrated the simulated for drop size distribution in other year 2007. It can be noted that the distribution of rain drop is more than that in 2003, where more light rain was fell compare to 2003. This is leading to the majority of the diameter of raindrops were small as result of larger amount of rain falling in the form of a light rain, with a little amount of middle raindrop diameter as result of middle rain.

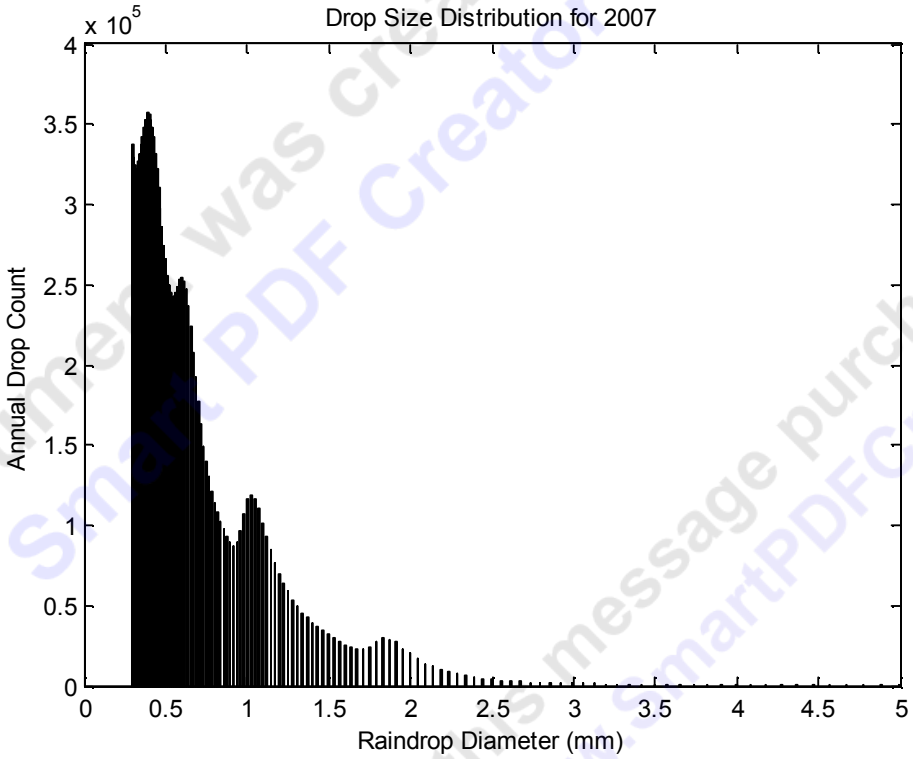

Figure 4.3 Drop Size Distribution for the year of 2007

In contrast of the that day which was chosen in the year of 2003, the Figure 4.4 shows that drop size distribution for a day which was chosen has a larger amount of raindrop diameter from about 0.3mm to 0.8mm for light rain.

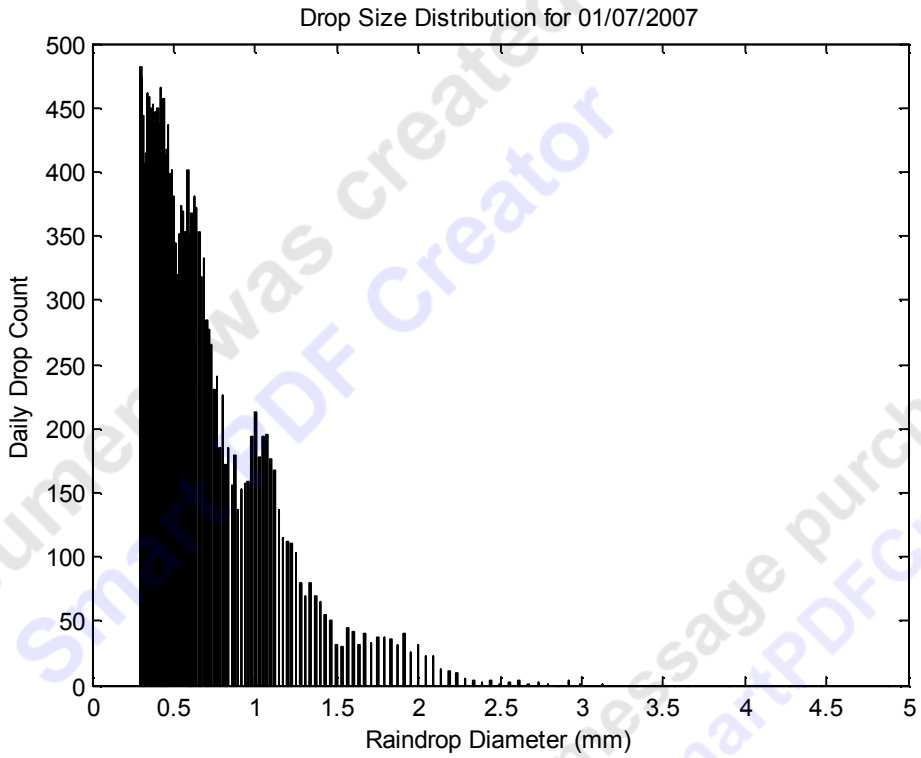

Figure 4.4 Drop Size Distribution for (01/07/2007)

Figure 4.5 is for this year 2010 which has data for first three month of year, the data are from 0mm to 5mm in raindrop diameter and from 0×10^4 to 9×10^4 in Annual drop count. The raindrop diameter for first three months of this year was also small. But with increasing in amount of diameter of raindrop more than a few last years as a result of a bit increasing of heavy rain.

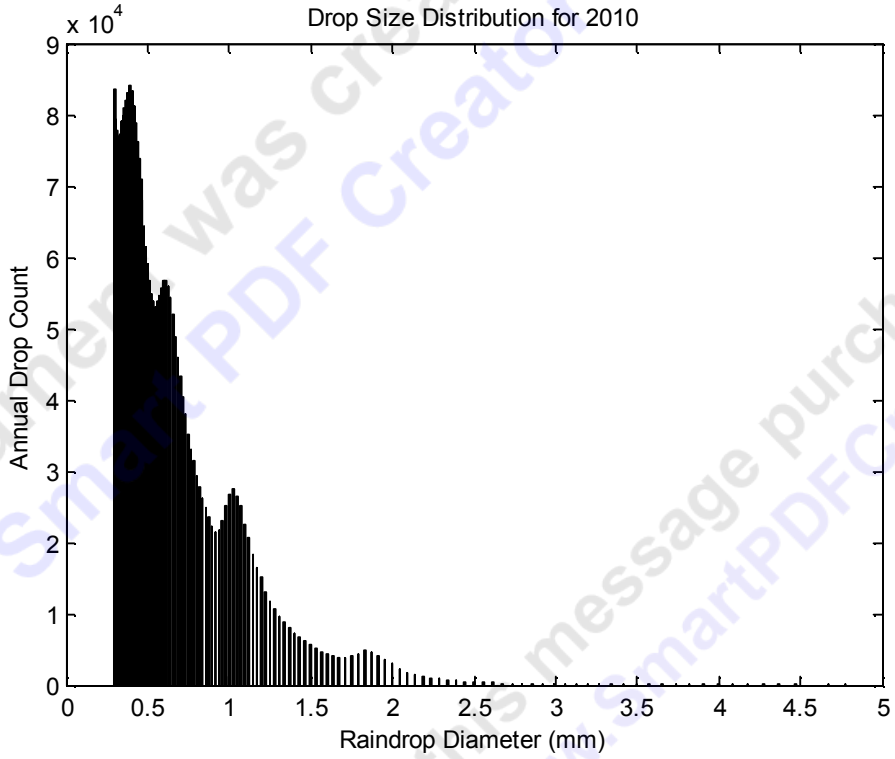

Figure 4.5 Drop Size Distribution for 2010

The simulated plot of the one day in Figure 4.6 below for a day on 22/01/2010 that was selected as a rainy day in this year. Which was light shower in that day, that led to the big amount of rain was small raindrop diameter,

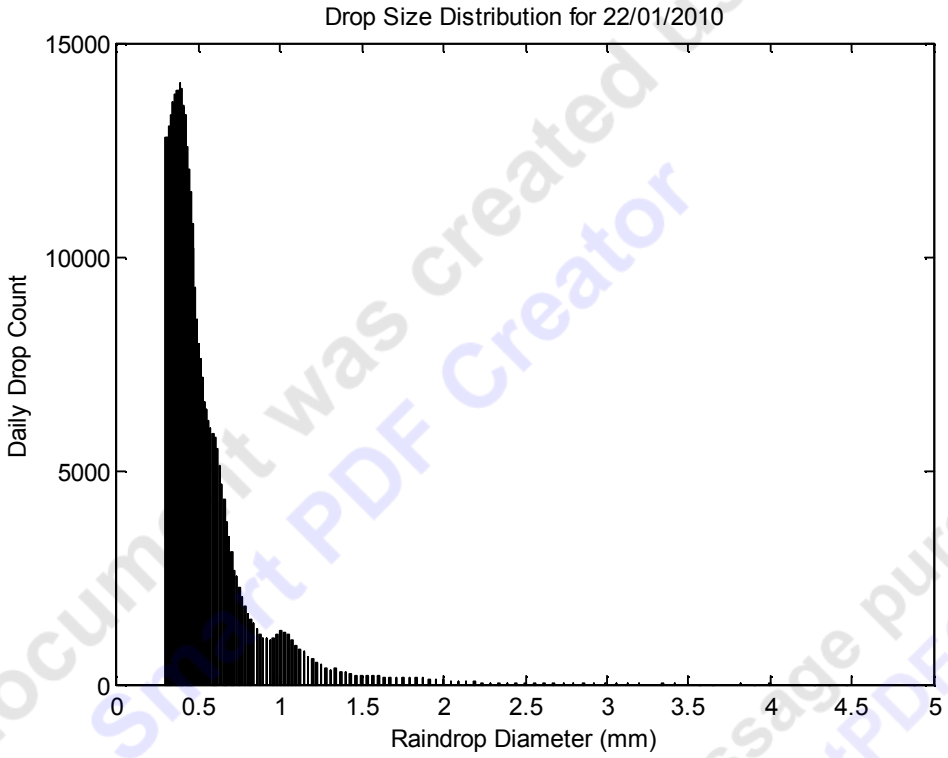

Figure 4.6 Drop Size Distribution for (22/01/2010)

Also by using Sparsholt site data which was started from 2004 until March 2010. The main reason to use other site of data is to overcome the problems of massing data that has been faced in some of years in first site. The simulation result of this site is also similar to Chilolton site with a bit different in some of years that has missing data.

In conclude of this program the results are illustrated that, there is no evidence shows an increasing of amount of heavy rain within this period of time.

4.3 Combine Daily DSD

In this part of work the second program was to read and build a 2D array of daily DSD spanning many years to combine the result of first program. By convolution, annual DSD are formed and from this array plots of made of time series of the exceedance probability of drops of various diameters and annual coverage.

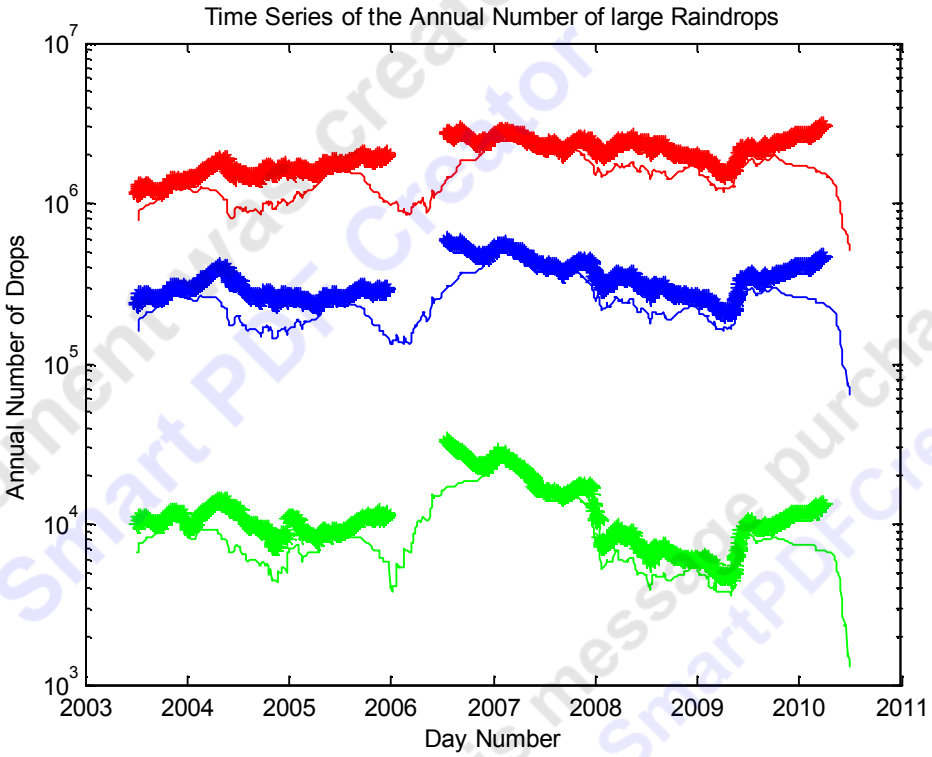

Figure 4.7 Time Series of the annual Number of large Raindrops

The first step in this program is to load the annual DSD data one year at a time and incorporate into the multi-year array. And then do a convolution to get running yearly coverage, then convolution to get running yearly accumulations of daily DSD. In order to know how many drops were of each diameter or bigger, this means turning DSD into an exceedance distribution.

The Figure above shows that the relationship between the size of raindrops and the annual number drops. The dark green line shows the number of drops in heaviest rain each day during all of period. The blue line illustrates the number of drops in middle heavy rain in each day. The red line illustrates the number of raindrops for light rain also in each day. In general, the number of drops that occurred as result of heavy rain is much lower than those that occur as a result of light rain.

In the other plot 4.8 illustrates the trend of annual coverage, middle day of year versus the proportion of year. From the graph as an example of year 2004, the proportion of middle day of year was 60%. Some of years have a high percentage of middle day and nearly to 99%. The biggest drop of trend was in a year of 2006, because the data has been massing for six month.

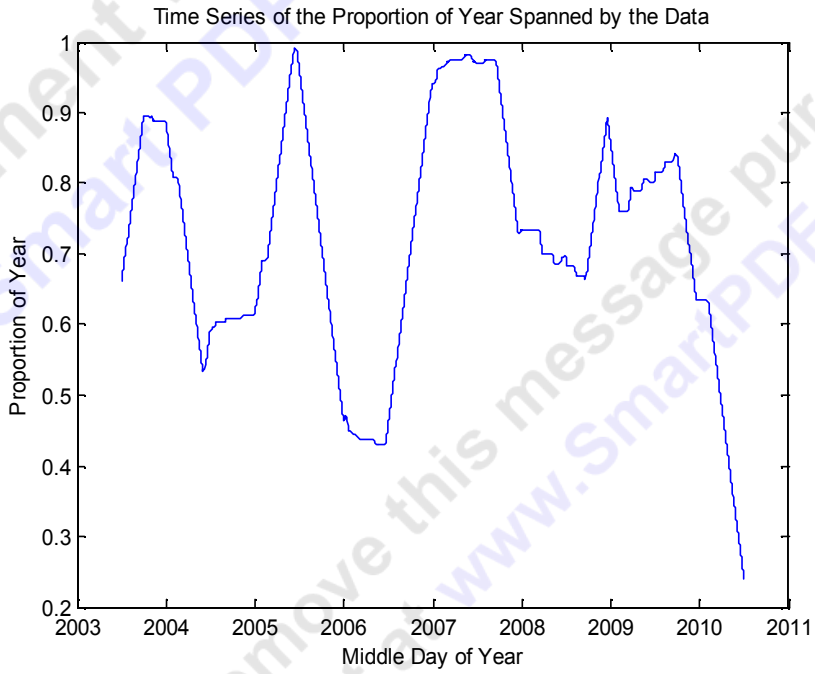

Figure 4.8 Time Series of the Proportion of Year Spanned by the Data

4.4 Trend Statistics

The aim of third program was to identify the trends in rain parameters for the same rate that affect microwave telecommunication links in time series data. Two statistical tests have been carried out (Man-Kendal and Person Correlation Coefficient). The results of both tests show that a number of drops decreases when the drop diameter is increasing more than 2mm. While this number of drops increases at the drop diameter less than approximately 2mm. This led to the majority number of rain drops is small as a result of light rain.

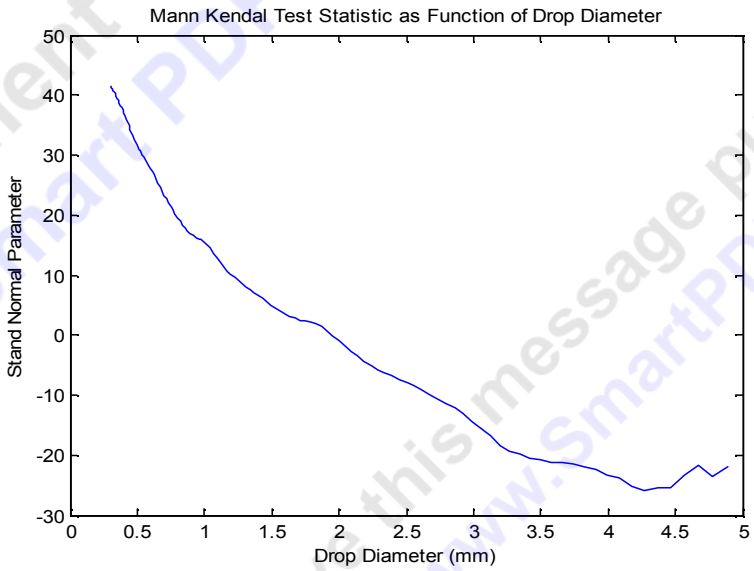

Figure 4.9 Mann Kendal Test Statistic as Function of Drop Diameter

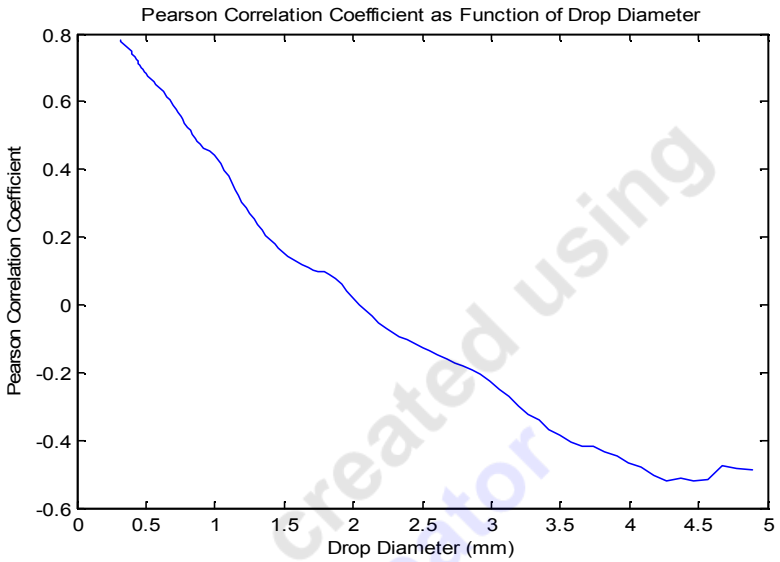

Figure 4.10 Pearson Correlation Coefficient as Function of Drop Diameter

4.5 Trends and probability Average of DSD for each Rain Rate

The last program was to identify trends and to calculate slope of exponential tail of associated DSD in different amount of rain rate within the period from 2005 to 2010. The annual exceedance probability of 10, 15, 20, 25, and 30 mm $^{-1}$ rain rates. These rain rate exceedances can be used to predict the performance of fixed links. It can see that the exponential parameter for Mann Kendall trend test and Person Correlation Trend test the probability did not give any provide evidence of an increasing trends that illustrate any change in the size of drops as a result of heavy rain.

The simulated plot of the Mean Diameter is shown in Figure 4.11. The majority of drops size for whole the period in different rain rate are small and no significant change in rain drop size can be seen within this period.

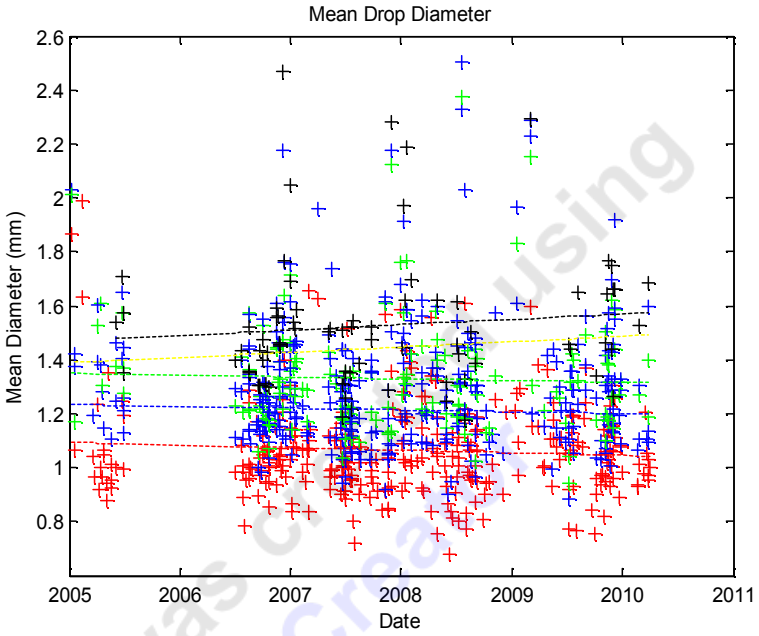

Figure 4.11 Mean Drop Diameter

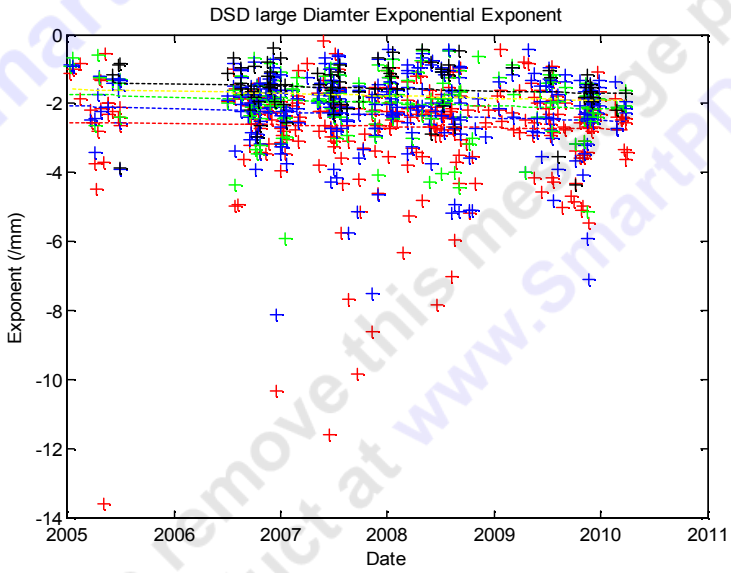

Figure 4.11 DSD large Diameter Exponential Exponent

CHAPTER 5

CONCLUSION AND FURTHER STUDY

5.1 Conclusion

In this thesis, there are several goals were originally stipulated to identify the effect of change in raindrops size distribution on the fixed terrestrial microwave links. Firstly, a drop size for each year was simulated to calculate daily and annual DSD with two different sits and the results compared. Secondly, all of these years were combined to be simulated with different kind of rain. Thirdly, two tests have been carried out to simulate the trends in rain parameters. Finally, the slope of exponential tail was calculated for various rain rates.

The simulation of DSD was illustrated the diameter of raindrops up to last six years. The results show that the all numbers of raindrops diameter were small as result of light rain, with very little number of middle drops diameter. A different of years were selected as an example and found the average of raindrop diameter approximately 1mm.

The result is combined to show time series of the annual number of large raindrops and proportion of year spanned by the data. The simulation software was used to determine the number of drops within all of period, then to show the diameter of raindrops. The results showed that the majority size of raindrops is small as a result of light rain with a little middle size of raindrops and very small number of big raindrops.

The rain parameter at the same rate was simulated to identify the trends by using two tests ((Man-Kendal and Person Correlation Coefficient). The results were found similar in both tests and to confirm that the numbers of drops increasing when the drop diameter is small and decreasing contrast. The last simulation software was to show any change in the raindrop size.

Therefore it can be concluded that:

- The results of computer simulation which is analysed the rain gauge data from two sites spanning for last 7 years showed that there is no significant change and no increase in the raindrop size in the UK as increase in the incidence of heavy rain events.
- This is leading to provide that there is no dramatic effect on microwave links that impact on the outage over the period 2003-2010. Also there is no increase interference in adjacent co-channel links. It is possible that these trends increase for the next few decades.
- The scattering cross section at microwave frequencies is proportional to the diameter of raindrops. Therefore, the specific attenuation is very sensitive to the number of large drops.
- The trends in rain fades in this work did not increase as a result of increasing in heavy rain.

5.2 Further Study

In this thesis as a future work to obtain results as predict effects of DSD changes that requires to be access in rain gauge data from good sites without any data massing. Also further analysis and statistics of data are needed in several directions and duration of rain intervals at outage levels.

APPENDIX

MAIN PORGRAM CODE

1.

```
Path = 'C:\Abdul-Karim_DSD1';
YearString4 = '2010';
Day1 = datenum( [ str2num(YearString4) 1 1 0 0 0 ] ) -
1;              % offset from day number to first day of year

cd( [ Path '\' YearString4 ] );
WildCard_FileName = [ 'cfarr-disdrometer_sparsholt_' YearString4
'*.nc' ];

Files = dir(WildCard_FileName);      % find all the files from the
year specified
[NumFiled NumFiles] = size( struct2cell(Files) );

% Declare arrays to hold daily DSD and coverage information
DailyDSD = zeros(127,366);             % 366 to allow for leap years
Coverage = zeros(366,1);

for iFile = 1:NumFiles

    Filename = Files(iFile).name;
    S = netcdf( Filename );

    MonthStr = Filename(33:34);
    DayStr = Filename(35:36);
    DayNumber = datenum( [ str2num(YearString4) str2num(MonthStr)
str2num(DayStr) 0 0 0 ] ) - Day1;

    DSD = S.VarArray(6).Data;

    Index = find( DSD == -999 );       % identify missing data
    if isempty(Index)
        Coverage(DayNumber) = 1.0;
    else
        DSD(Index) = 0;
        Coverage(DayNumber) = 1.0 - length(Index)/(24*60*6*127);
    end
    DailyDSD(:,DayNumber) = sum( DSD , 1 );

end

% just as an example do a drop size histogram
DropSize = S.VarArray(2).Data;
bar(DropSize,DailyDSD(:,22));
xlabel('Raindrop Diameter (mm)');
ylabel('Daily Drop Count');
title('Drop Size Distribution for 22/01/2010');

figure(2)
```

```
AnnualDSD = sum(DailyDSD,2);
bar(DropSize,AnnualDSD);
xlabel('Raindrop Diameter (mm)');
ylabel('Annual Drop Count');
title('Drop Size Distribution for 2010');

% Output to Mat file
OutPutFileName = [ Path '\DailyDSD' YearString4 ];
save(OutPutFileName, 'DailyDSD', 'Coverage');
```

2.

```
Path = 'C:\Abdul-Karim_DSD1';
YearString4 = '2010';
Day1 = datenum( [ str2num(YearString4) 1 1 0 0 0 ] ) -
1;              % offset from day number to first day of year

cd( [ Path '\' YearString4 ] );
WildCard_FileName = [ 'cfarr-disdrometer_chilbolton_' YearString4
'*.nc' ];
%WildCard_FileName = [ 'cfarr-disdrometer_sparsholt_' YearString4
'*.nc' ];

Files = dir(WildCard_FileName);        % find all the files from the
year specified
[NumFiled NumFiles] = size( struct2cell(Files) );

% Declare arrays to hold daily DSD and coverage information
DailyDSD = zeros(127,366);              % 366 to allow for leap years
Coverage = zeros(366,1);

for iFile = 1:NumFiles

    Filename = Files(iFile).name;
    S = netcdf( Filename );

    MonthStr = Filename(34:35);
    DayStr = Filename(36:37);
    DayNumber = datenum( [ str2num(YearString4) str2num(MonthStr)
str2num(DayStr) 0 0 0 ] ) - Day1;

    DSD = S.VarArray(6).Data;

    Index = find( DSD == -999 );        % identify missing data
    if isempty(Index)
        Coverage(DayNumber) = 1.0;
    else
        DSD(Index) = 0;
        Coverage(DayNumber) = 1.0 - length(Index)/(24*60*6*127);
    end
    DailyDSD(:,DayNumber) = sum( DSD , 1 );

end

% just as an example do a drop size histogram
DropSize = S.VarArray(2).Data;
bar(DropSize,DailyDSD(:,22));
xlabel('Raindrop Diameter (mm)');
```

```
ylabel('Daily Drop Count');
title('Drop Size Distribution for 22/01/2010');

figure(2)
AnnualDSD = sum(DailyDSD,2);
bar(DropSize,AnnualDSD);
xlabel('Raindrop Diameter (mm)');
ylabel('Annual Drop Count');
title('Drop Size Distribution for 2010');

% Output to Mat file
OutPutFileName = [ Path '\DailyDSD' YearString4 ];
save(OutPutFileName, 'DailyDSD', 'Coverage');
```

3.

```
Path = 'C:\Abdul-Karim_DSD1\';
cd(Path);
% load the annual DSD data one year at a time and incorporate into the
% multi-year array

% First File
FileName = [ Path 'DailyDSD2003.mat'];
load(FileName);
MultiYearDSD = DailyDSD(:,1:365);
MultiYearCoverage = Coverage(1:365);

% Next File (this time a leap year)
FileName = [ Path 'DailyDSD2004.mat'];
load(FileName);
MultiYearDSD = [ MultiYearDSD DailyDSD(:,1:366) ];
MultiYearCoverage = [ MultiYearCoverage ; Coverage(1:366) ];

% Next File
FileName = [ Path 'DailyDSD2005.mat'];
load(FileName);
MultiYearDSD = [ MultiYearDSD DailyDSD(:,1:365) ];
MultiYearCoverage = [ MultiYearCoverage ; Coverage(1:365) ];

% Next File
FileName = [ Path 'DailyDSD2006.mat'];
load(FileName);
MultiYearDSD = [ MultiYearDSD DailyDSD(:,1:365) ];
MultiYearCoverage = [ MultiYearCoverage ; Coverage(1:365) ];

% Next File
FileName = [ Path 'DailyDSD2007.mat'];
load(FileName);
MultiYearDSD = [ MultiYearDSD DailyDSD(:,1:365) ];
MultiYearCoverage = [ MultiYearCoverage ; Coverage(1:365) ];

% Next File (this time a leap year)
FileName = [ Path 'DailyDSD2008.mat'];
load(FileName);
MultiYearDSD = [ MultiYearDSD DailyDSD(:,1:366) ];
MultiYearCoverage = [ MultiYearCoverage ; Coverage(1:366) ];

% Next File
```

```
FileName = [ Path 'DailyDSD2009.mat'];
load(FileName);
MultiYearDSD = [ MultiYearDSD DailyDSD(:,1:365) ];
MultiYearCoverage = [ MultiYearCoverage ; Coverage(1:365) ];

% Next File
FileName = [ Path 'DailyDSD2010.mat'];
load(FileName);
MultiYearDSD = [ MultiYearDSD DailyDSD(:,1:365) ];
MultiYearCoverage = [ MultiYearCoverage ; Coverage(1:365) ];


% Do a convolution to get running yearly coverage
RunningAnnualCoverage =
conv2(MultiYearCoverage,ones(365,1)/365,'valid');

% Now do convolution to get running yearly accumulations of daily DSD
RunningAnnualDSD = conv2(MultiYearDSD,ones(1,365),'valid');


RunningAnnualDSD_XCD = cumsum(RunningAnnualDSD);

% This is close; this is a running sum over diamter bins.  But we want
the
% compliment of this.
for iRow = 1:127
    RunningAnnualDSD_XCD(iRow,:) = RunningAnnualDSD_XCD(127,:) -
RunningAnnualDSD_XCD(iRow,:);
end

% Form a vector of days in daynum format
DayNumber = (0:length(MultiYearCoverage)-1) + datenum( [ 2003 1 1 0 0
0 ] );
% Form a vector of the year centres
YearCentre = conv2(DayNumber,ones(1,365)/365,'valid');

% Now plot the time series of several drop diamter exceedances

figure(1)
semilogy(YearCentre,RunningAnnualDSD_XCD(50,:),'r')
hold on
semilogy(YearCentre,RunningAnnualDSD_XCD(75,:),'b')
semilogy(YearCentre,RunningAnnualDSD_XCD(100,:),'g')
xlabel('Day Number')
ylabel('Annual Number of Drops')
title('Time Series of the Annual Number of large Raindrops')
datetick('x',10)

% Now plot annual coverage

figure(2)
plot(YearCentre, RunningAnnualCoverage)
xlabel('Middle Day of Year')
ylabel('Proportion of Year')
title('Time Series of the Proportion of Year Spanned by the Data')
datetick('x',10)

% allow for time-series change of coverage
```

```
Index = find( RunningAnnualCoverage > 0.5 );
DSD_XCD_50 =
RunningAnnualDSD_XCD(50,Index)./RunningAnnualCoverage(Index)';
DSD_XCD_75 =
RunningAnnualDSD_XCD(75,Index)./RunningAnnualCoverage(Index)';
DSD_XCD_100 =
RunningAnnualDSD_XCD(100,Index)./RunningAnnualCoverage(Index)';

figure(1)
semilogy(YearCentre(Index), DSD_XCD_50','r*')
semilogy(YearCentre(Index), DSD_XCD_75','b*')
semilogy(YearCentre(Index), DSD_XCD_100','g*')
```

4.

```
Path = 'C:\Abdul-Karim_DSD1\';
cd(Path);
% load the annual DSD data one year at a time and incorporate into the
% multi-year array

% get drop diamter bin edges
S = netcdf( [Path '10\cfarr-disdrometer_chilbolton_20081001.nc'] );
DropDiameter = S.VarArray(2).Data;

% First File
FileName = [ Path 'DailyDSD2004.mat'];
load(FileName);
MultiYearDSD = DailyDSD(:,1:366);
MultiYearCoverage = Coverage(1:366);

% Next File (this time a leap year)
FileName = [ Path 'DailyDSD2005.mat'];
load(FileName);
MultiYearDSD = [ MultiYearDSD DailyDSD(:,1:365) ];
MultiYearCoverage = [ MultiYearCoverage ; Coverage(1:365) ];

% Next File
FileName = [ Path 'DailyDSD2006.mat'];
load(FileName);
MultiYearDSD = [ MultiYearDSD DailyDSD(:,1:365) ];
MultiYearCoverage = [ MultiYearCoverage ; Coverage(1:365) ];

% Next File
FileName = [ Path 'DailyDSD2007.mat'];
load(FileName);
MultiYearDSD = [ MultiYearDSD DailyDSD(:,1:365) ];
MultiYearCoverage = [ MultiYearCoverage ; Coverage(1:365) ];

% Next File
FileName = [ Path 'DailyDSD2008.mat'];
load(FileName);
MultiYearDSD = [ MultiYearDSD DailyDSD(:,1:366) ];
MultiYearCoverage = [ MultiYearCoverage ; Coverage(1:366) ];

% Next File (this time a leap year)
FileName = [ Path 'DailyDSD2009.mat'];
load(FileName);
```

```
MultiYearDSD = [ MultiYearDSD DailyDSD(:,1:365) ];
MultiYearCoverage = [ MultiYearCoverage ; Coverage(1:365) ];

% Next File
FileName = [ Path 'DailyDSD2010.mat'];
load(FileName);
MultiYearDSD = [ MultiYearDSD DailyDSD(:,1:365) ];
MultiYearCoverage = [ MultiYearCoverage ; Coverage(1:365) ];
% Do a convolution to get running yearly coverage
RunningAnnualCoverage =
conv2(MultiYearCoverage,ones(365,1)/365,'valid');

% Now do convolution to get running yearly accumulations of daily DSD
RunningAnnualDSD = conv2(MultiYearDSD,ones(1,365),'valid');

 nningAnnualDSD_XCD = cumsum(RunningAnnualDSD);

% This is close; this is a running sum over diamter bins.  But we want
the
% compliment of this.
nBin = 127;
for iRow = 1:nBin
    RunningAnnualDSD_XCD(iRow,:) = RunningAnnualDSD_XCD(nBin,:) -
RunningAnnualDSD_XCD(iRow,:);
end

% Form a vector of days in daynum format
DayNumber = (0:length(MultiYearCoverage)-1) + datenum( [ 2004 1 1 0 0
0 ] );
% Form a vector of the year centres
YearCentre = conv2(DayNumber,ones(1,365)/365,'valid');

% Now plot the time series of several drop diamter exceedances

figure(1)
semilogy(YearCentre,RunningAnnualDSD_XCD(50,:),'r')
hold on
semilogy(YearCentre,RunningAnnualDSD_XCD(75,:),'b')
semilogy(YearCentre,RunningAnnualDSD_XCD(100,:),'g')
xlabel('Day Number')
ylabel('Annual Number of Drops')
title('Time Series of the Annual Number of large Raindrops')
datetick('x',10)

% Now plot annual coverage

figure(2)
plot(YearCentre, RunningAnnualCoverage)
xlabel('Middle Day of Year')
ylabel('Proportion of Year')
title('Time Series of the Proportion of Year Spanned by the Data')
datetick('x',10)

% allow for time-series change of coverage

Index = find( RunningAnnualCoverage > 0.5 );
DSD_XCD_50 =
RunningAnnualDSD_XCD(50,Index)./RunningAnnualCoverage(Index)';
```

```
DSD_XCD_75 =
RunningAnnualDSD_XCD(75,Index)./RunningAnnualCoverage(Index)';
DSD_XCD_100 =
RunningAnnualDSD_XCD(100,Index)./RunningAnnualCoverage(Index)';

figure(1)
semilogy(YearCentre(Index), DSD_XCD_50','r*')
semilogy(YearCentre(Index), DSD_XCD_75','b*')
semilogy(YearCentre(Index), DSD_XCD_100','g*')

% Do Mann_Kendall tests
disp('Mann_Kendall and Pearson Correlation tests');

MKz = zeros(nBin,1);
PCr = zeros(nBin,1);

for iBin = 1:nBin
    disp([' Bin ' num2str(iBin) ]);

    SampleTime = YearCentre(Index);
    DSD_XCD_i =
RunningAnnualDSD_XCD(iBin,Index)./RunningAnnualCoverage(Index)';

    Z = Mann_Kendall_Trend_Test(DSD_XCD_i);
    if Z<0
        ProbThisBigByChance = 2*normcdf(Z,0,1);
 else
     ProbThisBigByChance = 2*normcdf(-Z,0,1);
    end
    disp( [ 'Z=' num2str(Z) '  with probabiity of exceedance by chance
' num2str( ProbThisBigByChance ) ] );

    [R,P] = corrcoef(SampleTime,DSD_XCD_i);
    ProbThisBigByChance = P(1,2);
    disp( [ 'R=' num2str(R(1,2)) '  with probabiity of exceedance by
chance ' num2str( ProbThisBigByChance ) ] );

    MKz(iBin) = Z;
    PCr(iBin) = R(1,2);


end

% Now plot trend statistics


figure(3)
plot(DropDiameter(1:126), MKz(1:126))
xlabel('Drop Diameter (mm)')
ylabel('Stand Normal Parameter')
title('Mann Kendal Test Statistic as Function of Drop Diameter')

figure(4)
plot(DropDiameter(1:126), PCr(1:126))
xlabel('Drop Diameter (mm)')
ylabel('Pearson Correlation Coefficient')
title('Pearson Correlation Coefficient as Function of Drop Diameter')
```

5.

```
% Mann_Kendal_Trend_Test

function [Z] = Mann_Kendall_Trend_Test(X)

nX = length(X);

P = 0;
M = 0;
for iX = 1:nX-1
    for jX = iX+1:nX
        if X(iX)>X(jX)
            P = P+1;
        else
            M = M+1;
        end
    end
end
S=M-P;

Standard_Deviation = sqrt( nX*(nX-1)*(2*nX+5)/18 );
if S > 0
    Z = (S-1)/Standard_Deviation;
elseif S<0
    Z = (S+1)/Standard_Deviation;
else
    Z = 0;
end
```

6.

```
DistArea = 50 * 100;            % catchment area of Joss Disdrometer in
mm^2
MinD = 80;

Path = 'C:\Abdul-Karim_DSD1';
YearString4 = '2010';
Day1 = datenum( [ str2num(YearString4) 1 1 0 0 0 ] ) - 1;               %
offset from day number to first day of year

cd( [ Path '\' YearString4 ] );
WildCard_FileName = [ 'cfarr-disdrometer_chilbolton_' YearString4 '*.nc' ];
Files = dir(WildCard_FileName);       % find all the files from the year
specified
[NumFiled NumFiles] = size( struct2cell(Files) );

% Declare arrays to hold daily DSD and coverage information
TargetRainRates = 10:5:50;
nRainRate = length( TargetRainRates );
DeltaRainRate = 2.5;
RainRateDSD_exp = ones(nRainRate,366)*999;              % 366 to allow for
leap years
RainRateDSD_mean = ones(nRainRate,366)*(-999);             % 366 to allow
for leap years

First = true;
```

```
for iFile = 1:NumFiles

    Filename = Files(iFile).name;
    S = netcdf( Filename );

    MonthStr = Filename(34:35);
    DayStr = Filename(36:37);
    DayNumber = datenum( [ str2num(YearString4) str2num(MonthStr)
str2num(DayStr) 0 0 0 ] ) - Day1;

    DSD = S.VarArray(6).Data;
    DSD( DSD<0 ) = 0;
    DSD = double(DSD );

    % work out rain rates
    if First                % first time through get drop sizes
        First = false;
        DropSize = S.VarArray(2).Data;
        % work out drop volume array for conversion of DSD to rain rate
        DSD_to_RainRate = pi/6*DropSize.^3 / DistArea *60;
    end

    DSD60 = conv2(DSD,ones(6,1),'valid');
    RainRate60 = DSD60 * DSD_to_RainRate;

    % Loop over target rain rates and calculate slope of exponential tail
    % of associated DSD.

    for iRR = 1:nRainRate

        Index = find( abs(RainRate60-TargetRainRates(iRR)) <
DeltaRainRate );
        if ~isempty(Index)
            DSD_RR = sum(DSD60(Index,:),1);

            % fit exponential to tail
            FitDropSize = DropSize(MinD:end);
            Fit_DSD_RR = DSD_RR(MinD:end)';
            Index = find( Fit_DSD_RR > 0 );
             p = polyfit( FitDropSize(Index) , log(Fit_DSD_RR(Index)),1);
             RainRateDSD_exp(iRR,DayNumber) = p(1);
             RainRateDSD_mean(iRR,DayNumber) = DSD_RR*DropSize/sum(DSD_RR);

             if false
                 plot( FitDropSize(Index) , log(Fit_DSD_RR(Index)) );
                 title( [ Filename num2str(iRR) ] );
                 hold on
                 plot( FitDropSize(Index) , p(2) + p(1)*FitDropSize(Index) ,
'r--' );
                 hold off
             end
        end

    end

end
```

```
% Output to Mat file
OutPutFileName = [ Path '\DailyDSD_Exponents' YearString4 ];
save(OutPutFileName, 'RainRateDSD_exp' , 'RainRateDSD_mean' );
```

7.

```
Path = 'C:\Abdul-Karim_DSD1\';

% load the annual DSD data one year at a time and incorporate into the
% multi-year array

% First File
FileName = [ Path 'DailyDSD_Exponents2005'];
load(FileName);
MultiYearDSD_exp = RainRateDSD_exp(:,1:365);
MultiYearDSD_mean = RainRateDSD_mean(:,1:365);
DayDate = datenum([2005 1 1 0 0 0 ]) + (0:364);

% Next File (remember to deal with leap years)
FileName = [ Path 'DailyDSD_Exponents2006'];
load(FileName);
MultiYearDSD_exp = [ MultiYearDSD_exp RainRateDSD_exp(:,1:365) ];
MultiYearDSD_mean = [ MultiYearDSD_mean RainRateDSD_mean(:,1:365) ];
DayDate = [ DayDate datenum([2006 1 1 0 0 0 ]) + (0:364) ];

% Next File (remember to deal with leap years)
FileName = [ Path 'DailyDSD_Exponents2007'];
load(FileName);
MultiYearDSD_exp = [ MultiYearDSD_exp RainRateDSD_exp(:,1:365) ];
MultiYearDSD_mean = [ MultiYearDSD_mean RainRateDSD_mean(:,1:365) ];
DayDate = [ DayDate datenum([2007 1 1 0 0 0 ]) + (0:364) ];

% Next File (remember to deal with leap years)
FileName = [ Path 'DailyDSD_Exponents2008'];
load(FileName);
MultiYearDSD_exp = [ MultiYearDSD_exp RainRateDSD_exp(:,1:366) ];
MultiYearDSD_mean = [ MultiYearDSD_mean RainRateDSD_mean(:,1:366) ];
DayDate = [ DayDate datenum([2008 1 1 0 0 0 ]) + (0:365) ];

% Next File (remember to deal with leap years)
FileName = [ Path 'DailyDSD_Exponents2009'];
load(FileName);
MultiYearDSD_exp = [ MultiYearDSD_exp RainRateDSD_exp(:,1:365) ];
MultiYearDSD_mean = [ MultiYearDSD_mean RainRateDSD_mean(:,1:365) ];
DayDate = [ DayDate datenum([2009 1 1 0 0 0 ]) + (0:364) ];

% Next File (remember to deal with leap years)
FileName = [ Path 'DailyDSD_Exponents2010'];
load(FileName);
MultiYearDSD_exp = [ MultiYearDSD_exp RainRateDSD_exp(:,1:365) ];
MultiYearDSD_mean = [ MultiYearDSD_mean RainRateDSD_mean(:,1:365) ];
DayDate = [ DayDate datenum([2010 1 1 0 0 0 ]) + (0:364) ];

% Now plot the time series of DSD exponents for a range of rain rates

figure(1)
% RainRate = 10 mm/hr
Index = find( MultiYearDSD_exp(1,:) < 0 );
plot(DayDate(Index), MultiYearDSD_exp(1,Index) , 'r+' )
```

```
hold on
% RainRate = 15 mm/hr
Index = find( MultiYearDSD_exp(2,:) < 0 );
plot(DayDate(Index), MultiYearDSD_exp(2,Index) , 'b+' )
% RainRate = 20 mm/hr
Index = find( MultiYearDSD_exp(3,:) < 0 );
plot(DayDate(Index), MultiYearDSD_exp(3,Index) , 'g+' )
% RainRate = 25 mm/hr
Index = find( MultiYearDSD_exp(4,:) < 0 );
plot(DayDate(Index), MultiYearDSD_exp(4,Index) , 'b+' )
% RainRate = 30 mm/hr
Index = find( MultiYearDSD_exp(5,:) < 0 );
plot(DayDate(Index), MultiYearDSD_exp(5,Index) , 'k+' )

xlabel('Date')
ylabel('Exponent (/mm)')
title('DSD large Diamter Exponential Exponent')
datetick('x',10)

% Now plot the time series of drop mean diamters for a range of rain rates

figure(2)
% RainRate = 10 mm/hr
Index = find( MultiYearDSD_mean(1,:) > 0 );
plot(DayDate(Index), MultiYearDSD_mean(1,Index) , 'r+' )
hold on
% RainRate = 15 mm/hr
Index = find( MultiYearDSD_mean(2,:) > 0 );
plot(DayDate(Index), MultiYearDSD_mean(2,Index) , 'b+' )
% RainRate = 20 mm/hr
Index = find( MultiYearDSD_mean(3,:) > 0 );
plot(DayDate(Index), MultiYearDSD_mean(3,Index) , 'g+' )
% RainRate = 25 mm/hr
Index = find( MultiYearDSD_mean(4,:) > 0 );
plot(DayDate(Index), MultiYearDSD_mean(4,Index) , 'b+' )
% RainRate = 30 mm/hr
Index = find( MultiYearDSD_mean(5,:) > 0 );
plot(DayDate(Index), MultiYearDSD_mean(5,Index) , 'k+' )

xlabel('Date')
ylabel('Mean Diameter (mm)')
title('Mean Drop Diameter')
datetick('x',10)



figure(1)
% RainRate = 10 mm/hr
Index = find( MultiYearDSD_exp(1,:) < 0 );
p = polyfit( DayDate(Index), MultiYearDSD_exp(1,Index) , 1);
plot(DayDate(Index), p(2) + p(1)*DayDate(Index) , 'r--' )
% RainRate = 15 mm/hr
Index = find( MultiYearDSD_exp(2,:) < 0 );
p = polyfit( DayDate(Index), MultiYearDSD_exp(2,Index) , 1);
plot(DayDate(Index), p(2) + p(1)*DayDate(Index) , 'b--' )
% RainRate = 20 mm/hr
Index = find( MultiYearDSD_exp(3,:) < 0 );
p = polyfit( DayDate(Index), MultiYearDSD_exp(3,Index) , 1);
plot(DayDate(Index), p(2) + p(1)*DayDate(Index) , 'g--' )
% RainRate = 25 mm/hr
Index = find( MultiYearDSD_exp(4,:) < 0 );
```

```
p = polyfit( DayDate(Index), MultiYearDSD_exp(4,Index) , 1);
plot(DayDate(Index), p(2) + p(1)*DayDate(Index) , 'y--' )
% RainRate = 30 mm/hr
Index = find( MultiYearDSD_exp(5,:) < 0 );
p = polyfit( DayDate(Index), MultiYearDSD_exp(5,Index) , 1);
plot(DayDate(Index), p(2) + p(1)*DayDate(Index) , 'k--' )

% Now plot the time series of drop mean diamters for a range of rain rates

figure(2)
% RainRate = 10 mm/hr
Index = find( MultiYearDSD_mean(1,:) > 0 );
p = polyfit( DayDate(Index), MultiYearDSD_mean(1,Index) , 1);
plot(DayDate(Index), p(2) + p(1)*DayDate(Index) , 'r--' )
% RainRate = 15 mm/hr
Index = find( MultiYearDSD_mean(2,:) > 0 );
p = polyfit( DayDate(Index), MultiYearDSD_mean(2,Index) , 1);
plot(DayDate(Index), p(2) + p(1)*DayDate(Index) , 'b--' )
% RainRate = 20 mm/hr
Index = find( MultiYearDSD_mean(3,:) > 0 );
p = polyfit( DayDate(Index), MultiYearDSD_mean(3,Index) , 1);
plot(DayDate(Index), p(2) + p(1)*DayDate(Index) , 'g--' )
% RainRate = 25 mm/hr
Index = find( MultiYearDSD_mean(4,:) > 0 );
p = polyfit( DayDate(Index), MultiYearDSD_mean(4,Index) , 1);
plot(DayDate(Index), p(2) + p(1)*DayDate(Index) , 'y--' )
% RainRate = 30 mm/hr
Index = find( MultiYearDSD_mean(5,:) > 0 );
p = polyfit( DayDate(Index), MultiYearDSD_mean(5,Index) , 1);
plot(DayDate(Index), p(2) + p(1)*DayDate(Index) , 'k--' )


disp( ' Exponential Parameter' )

disp( ' Mann Kendall Trend Tests' )

% Mann Kendall Tests
disp( 'RainRate = 10 mm/hr' )
Z = Mann_Kendall_Trend_Test(MultiYearDSD_exp(1,MultiYearDSD_exp(1,:) < 0))
ProbThisBigByChance = 2*(1-normcdf(abs(Z),0,1))

disp( 'RainRate = 15 mm/hr' )
Z = Mann_Kendall_Trend_Test(MultiYearDSD_exp(2,MultiYearDSD_exp(2,:) < 0))
ProbThisBigByChance = 2*(1-normcdf(abs(Z),0,1))

disp( 'RainRate = 20 mm/hr' )
Z = Mann_Kendall_Trend_Test(MultiYearDSD_exp(3,MultiYearDSD_exp(3,:) < 0))
ProbThisBigByChance = 2*(1-normcdf(abs(Z),0,1))

disp( 'RainRate = 25 mm/hr' )
Z = Mann_Kendall_Trend_Test(MultiYearDSD_exp(4,MultiYearDSD_exp(4,:) < 0))
ProbThisBigByChance = 2*(1-normcdf(abs(Z),0,1))

disp( 'RainRate = 30 mm/hr' )
Z = Mann_Kendall_Trend_Test(MultiYearDSD_exp(5,MultiYearDSD_exp(5,:) < 0))
ProbThisBigByChance = 2*(1-normcdf(abs(Z),0,1))


disp( ' Pearson Correlation Trend Tests' )
```

```
% Pearson Correlation Trend Tests
disp( 'RainRate = 10 mm/hr' )
Index = find( MultiYearDSD_exp(1,:) < 0 );
[R,P] = corrcoef(DayDate(Index), MultiYearDSD_exp(1,Index))

disp( 'RainRate = 15 mm/hr' )
Index = find( MultiYearDSD_exp(2,:) < 0 );
[R,P] = corrcoef(DayDate(Index), MultiYearDSD_exp(2,Index))

disp( 'RainRate = 20 mm/hr' )
Index = find( MultiYearDSD_exp(3,:) < 0 );
[R,P] = corrcoef(DayDate(Index), MultiYearDSD_exp(3,Index))

disp( 'RainRate = 25 mm/hr' )
Index = find( MultiYearDSD_exp(4,:) < 0 );
[R,P] = corrcoef(DayDate(Index), MultiYearDSD_exp(4,Index))

disp( 'RainRate = 30 mm/hr' )
Index = find( MultiYearDSD_exp(5,:) < 0 );
[R,P] = corrcoef(DayDate(Index), MultiYearDSD_exp(5,Index))


disp( ' Mean Drop Diameter' )

disp( ' Mann Kendall Trend Tests' )

% Mann Kendall Tests
disp( 'RainRate = 10 mm/hr' )
Z = Mann_Kendall_Trend_Test(MultiYearDSD_mean(1,MultiYearDSD_mean(1,:) > 0))
ProbThisBigByChance = 2*(1-normcdf(abs(Z),0,1))

disp( 'RainRate = 15 mm/hr' )
Z = Mann_Kendall_Trend_Test(MultiYearDSD_mean(2,MultiYearDSD_mean(2,:) > 0))
ProbThisBigByChance = 2*(1-normcdf(abs(Z),0,1))

disp( 'RainRate = 20 mm/hr' )
Z = Mann_Kendall_Trend_Test(MultiYearDSD_mean(3,MultiYearDSD_mean(3,:) > 0))
ProbThisBigByChance = 2*(1-normcdf(abs(Z),0,1))

disp( 'RainRate = 25 mm/hr' )
Z = Mann_Kendall_Trend_Test(MultiYearDSD_mean(4,MultiYearDSD_mean(4,:) > 0))
ProbThisBigByChance = 2*(1-normcdf(abs(Z),0,1))

disp( 'RainRate = 30 mm/hr' )
Z = Mann_Kendall_Trend_Test(MultiYearDSD_mean(5,MultiYearDSD_mean(5,:) > 0))
ProbThisBigByChance = 2*(1-normcdf(abs(Z),0,1))


disp( ' Pearson Correlation Trend Tests' )

% Pearson Correlation Trend Tests
disp( 'RainRate = 10 mm/hr' )
Index = find( MultiYearDSD_mean(1,:) > 0 );
[R,P] = corrcoef(DayDate(Index), MultiYearDSD_mean(1,Index))

disp( 'RainRate = 15 mm/hr' )
Index = find( MultiYearDSD_mean(2,:) > 0 );
```

```
[R,P] = corrcoef(DayDate(Index), MultiYearDSD_mean(2,Index))

disp( 'RainRate = 20 mm/hr' )
Index = find( MultiYearDSD_mean(3,:) > 0 );
[R,P] = corrcoef(DayDate(Index), MultiYearDSD_mean(3,Index))

disp( 'RainRate = 25 mm/hr' )
Index = find( MultiYearDSD_mean(4,:) > 0 );
[R,P] = corrcoef(DayDate(Index), MultiYearDSD_mean(4,Index))

disp( 'RainRate = 30 mm/hr' )
Index = find( MultiYearDSD_mean(5,:) > 0 );
[R,P] = corrcoef(DayDate(Index), MultiYearDSD_mean(5,Index))
```

References

Andsager, K., Beard, K. V. and Laird, N. F. (1999). "Laboratory measurements of axis ratios for large raindrops". *Journal of the Atmospheric Sciences*, volume 56, pp. 2673–2683,

Atlas, D., Ulbrich, C.W. and Meneghini, R. (1984). "The multiparameter remote measurement of rainfall". *Radio Science*, volume 19(1), pp. 3–22.

Atlas, D. and Ulbrich, C. W (1977) "Path- and area-integrated rainfall measurement by microwave attenuation in the 1-3cm band", *Journal of Applied Meteorology*, *16*, 1322-1331.

Beard, K. V. and Chuang, C. (1987). "A new model for the equilibrium shape of raindrops*"*. *Journal of the Atmospheric Sciences*, volume 44(11), pp. 1509 – 1524,

Crane, R. K. (1980). "Prediction of attenuation by rain," *IEEE Transactions on Communications,* vol. 28, n. 9, Sep. pp. 1117-1133,

Defra, 2001. "National appraisal of assets at risk from flooding and coastal erosion", including the potential impact of climate change. DEFRA Technical Report.

Goddard, J.W. F. and Cherry, S. M. (1984). "The ability of dual-polarisation radar (copolar linear)to predict rainfall rate and microwave attenuation." *Radio Science*, volume 19(1), pp. 201–208,

Hardaker, P. J., Holt, A. R. and Goddard, J. W. F. (1997), "Comparing model and measured rainfall rates obtained from a combination of remotely sensed and in situ observations," *Radio Science*, Vol. 32, No. (5), pp. 1785–96.

Jameson, A. R., A, (1991). "comparison of microwave techniques for measuring rainfall", *Journal of Applied Meteorology*, 30, 32-54,

Jiang,H. and Sano, M. (1996). "Radar reftectivity and rainfall rate relation from Weibull raindrop-size distribution," *IEICE Trans. Commun.,* vol. E79-B, Jun. n. 6.

Jiang,H. and Sano,M. and Sekine, M.(1997) "Weibull raindropsize distribution and its application to rain attenuation ." *IEE Proceedings Microwaves. Antennas, and Propagation,* vol. 144. n. 3. Jun. pp. 197-200.

Lawrimore, J.H., Halpert, M.S., Bell, G.D., Menne, M.J., Lyon, B., Schnell, R.C., Gleason, K.L., Easterling, D.R., Thiaw, W., Wright, W.J., Heim, R.R., Robinson, D.A., Alexander, L., (2001), "Climate assessment for 2000". *Bulletin of the American Meteorological Society* 82, S1 S62.

Laws, J. and Parsons, D. (1943), "The relation of rain drop size to intensity," *Transactions of the American Geophysical Union*, Vol. 24, No. (2), pp. 452–460

Lin, S. H. (1975). "A method for calculating rain attenuation distributions on microwave" paths:' *Bell Syst. Tech. J.,* vol 54,n.6,pp. 1051-1086.

Lutgens, F. K. and Tarbuck,E. J. (2001), *The atmosphere,* 8th ed., Prentice Hall, New Jersey.

Marshall, J. and Palmer, W. (1948), "The distribution of rain drop with size," *Journal of meteorology*, Vol. 5, pp 165–166.

Oguchi, T.(1960). "Attenuation of electromagnetic wave due to rain with distorted raindrops," *Journal of the Radio Research lAboratories,* vol. 7, no. 33, Sep. pp. 467-485.

Oguchi, T. (1977). "Scattering properties of Pruppacher-and-Pitter form raindrops and cross polarization due to rain: Calculations at Il. 13, 19.3, and 34.8 GHz," *Radio Science,* vol. 12, n. l, Jan.-Feb. pp. 41-51.

Olsen, R. L. Rogers, D. V. and Hodge, D. B. (1978) "The aRb relation in the calculation of rain attenuation," *IEEE Transactions on Antennas &: Propagation.* vol. 26, Mar.n. 2, pp. 318-329.

Olsen, R. L. Rogers, D. V. and Hodge, D, B. (1981)."The aRb relation in the calculation of rain attenuation," *IEEE Transactions on Antennas &: Propagation.* vol. 26, n. 2, Mar. pp. 318-329.

Paulson, K. S. (2010) "Trends in the incidence of rain rates associated with outages on fixed links operating above 10GHz in the southern United Kingdom," *Radio Science,*Vol. 45, 23 February, pp. 9.

Pruppacher, H. R. and Beard, K. V. (1970). "A wind tunnel investigation of the internal circulation and shape of water drops falling at terminal velocity in air". *Quarterly Journal of the Royal Meteorological Society*, volume 96, pp. 247 – 256.

Rahimi, A., Upton, G. and Holt, A (2004), " Dual-frequency links-a complement to gauges and radar for the measurement of rain," *Journal of Hydrology,*Vol.288, No. (1-2), 20 March, pp. 3–12.

Rincon, R. F. and R. H. Lang,(2002). "Microwave link dual-wavelength measurements of path-average attenuation for the estimation of drop size distributions and rainfall," *IEEE Transactions on Geoscience and Remote Sensing*, *40(4)*, 760- 770.

Sekine,M. and Lind,G. (1982), "Rain attenuation of centimeter. millimeter and slJb-millimeter radio waves," *Proc. Ofthe /2th European microwave conference.* Helsinki, Finland. pp. 584-589.

Tokay, A. and Short, D. A.(1996). "Evidence from tropical raindrop spectra of the origin of rain from stratiform versus convective clouds". *Journal of Applied Meteorology*, volume 35(3), pp. 355–71.

Ulbrich, C.W.(1983). "Natural variations in the analytical form of the raindrop size distribution". *Journal of Climate and Applied Meteo*rology, volume 22(10), pp. 1764–75.

Williams, C. R., (2002), "Simultaneous ambient air motion and raindrop size distributions retrieved from UHF vertical incident profiler observations," *Radio Sci*., Vol. 37, No. 2.

http://www.coralcoe.org.au/research/simonpng/EEPL_1_acidrain.pdf accessed 13th July. 2010.

http://www.everythingweather.com/atmospheric-radiation/scattering.shtml accessed 5th August. 2010.